Environment International 202 (2025) 109583

Contents lists available at ScienceDirect

Environment International

journal homepage: www.elsevier.com/locate/envint

Full length article

Transported smoke from crop residue burning as the major source of organic aerosol and health risks in northern Indian cities during post-monsoon

Yufang Hao [a,*], Jan Strähl [b,c], Peeyush Khare [a,1], Tianqu Cui [a], Kristty Schneider-Beltran [a], Lu Qi [a], Dongyu Wang [a], Jens Top [a], Mihnea Surdu [a], Deepika Bhattu [a,2], Himadri Sekhar Bhowmik [d], Pawan Vats [e], Pragati Rai [a], Varun Kumar [a], Dilip Ganguly [e], Sönke Szidat [b,c], Gaëlle Uzu [f], Jean-Luc Jaffrezo [f], Rhabira Elazzouzi [f], Neeraj Rastogi [g], Jay Slowik [a], Imad EI Haddad [a], Sachchida Nand Tripathi [d], André S.H. Prévôt [a,*], Kaspar Rudolf Daellenbach [a,*]

[a] PSI Center for Energy and Environmental Sciences, Paul Scherrer Institute, 5232 Villigen, Switzerland
[b] Department of Chemistry, Biochemistry and Pharmaceutical Sciences, University of Bern 3012 Bern, Switzerland
[c] Oeschger Centre for Climate Change Research, University of Bern, 3012 Bern, Switzerland
[d] Department of Civil Engineering, Indian Institute of Technology Kanpur, 208016, India
[e] Centre for Atmospheric Sciences, Indian Institute of Technology Delhi, New Delhi 110016, India
[f] Université Grenoble Alpes, CNRS, IRD, G-INP, UMR 5001 IGE, 38000 Grenoble, France
[g] Geosciences Division, Physical Research Laboratory, Ahmedabad 380009, India

ARTICLE INFO

Handling Editor: Dr. Xavier Querol

Keywords:
Organic aerosol
Source apportionment
Molecular characterization
Biomass burning

ABSTRACT

Ambient particulate matter significantly impacts air quality, climate, and human health. In the Indo-Gangetic Plain (IGP), home to nearly one-seventh of the global population, severe air pollution is prevalent with high $PM_{2.5}$ levels dominated by organic aerosols (OA). However, the sources and formation of OA pollution remain poorly constrained. For the first time, we characterize OA sources in two cities, Delhi and Kanpur in the IGP, over an entire year by combining near-molecular characterizations using an extractive electrospray ionization time-of-flight mass spectrometer (EESI-TOF) with advanced statistical approaches. We identified three key local biomass burning sources—affected by various fuels such as wood, straw, and cow dung—that had a more pronounced impact on Kanpur (66 %) compared to Delhi (35 %), particularly during colder months. Additionally, we identified transported agricultural fire emissions from Northwest India, which significantly contributed to OA during the post-monsoon rice harvest season, playing a critical role in haze formation. Acute mortality estimates indicated that while urban OA sources were substantial, rural crop residue burning posed a notable health risk during the post-monsoon, accounting for 32 % of $PM_{2.5}$-attributable mortality in Delhi and 53 % in Kanpur. These results highlight the need for coordinated air pollution mitigation strategies that extend beyond urban centres to a regional scale, with a particular focus on crop residue management in Punjab to reduce the health burden of $PM_{2.5}$ pollution in the IGP.

1. Introduction

Ambient particulate matter (PM) pollution constitutes a major threat to public health, contributing to over 4 million premature deaths annually worldwide (WHO, 2021; Fuller et al., 2022; Sang et al., 2022). In India, long-term exposure to atmospheric particulate matter with aerodynamic diameter smaller than 2.5 μm ($PM_{2.5}$) alone was estimated to be responsible for nearly 1 million premature deaths in 2019, making

* Corresponding authors.
E-mail addresses: yufang.hao@psi.ch (Y. Hao), andre.prevot@psi.ch (A.S.H. Prévôt), kaspar.daellenbach@psi.ch (K.R. Daellenbach).
[1] Now at Institute of Climate and Energy Systems (ICE-3): Troposphere, Forschungszentrum Jülich, Germany.
[2] Now at Department of Civil and Infrastructure Engineering, Indian Institute of Technology Jodhpur, 342037, India

https://doi.org/10.1016/j.envint.2025.109583
Received 18 January 2025; Received in revised form 11 May 2025; Accepted 2 June 2025
Available online 3 June 2025

it one of the country's major environmental hazards (GBD 2019 Risk Factors Collaborators, 2020). The Indo-Gangetic Plain (IGP), home to about one-seventh of the world's population, frequently experiences exceptionally high $PM_{2.5}$ concentration, with levels reaching 900 μg m^{-3} during pollution episodes (Dutta and Chatterjee, 2022; Singh et al., 2023). Addressing this crisis requires a detailed understanding of $PM_{2.5}$ composition and sources to develop effective mitigation strategies.

Organic aerosols (OA), the dominant $PM_{2.5}$ component in the IGP, originate from both primary OA (POA) directly from emissions such as biomass burning and fuel combustion, and secondary OA (SOA) from atmospheric oxidation of volatile organic compounds (VOCs) (Jain et al., 2020; Gunthe et al., 2021; Patel et al., 2021). While urban sources such as traffic and industry degrade air quality in cities like Delhi (Rai et al., 2020; Maheshwarkar et al., 2022; Bhattu et al., 2024; Bhowmik et al., 2024a), rural contributions including household solid fuel use and post-harvest crop residue burning are also critical (Kulkarni et al., 2020; Lan et al., 2022; Pawar and Sinha, 2022). Secondary processes like aqueous-phase oxidation (Kumar et al., 2016; Rajput et al., 2018) or wintertime new particle formation (Gunthe et al., 2021; Mishra et al., 2023) have also been found to further exacerbate haze events. Yet, key challenges persist relating to characterizing the spatiotemporal variability of OA sources, distinguishing various POA, and quantifying complex SOA types. Specifically, rural agricultural fires are often identified as a major contributor to pollution episodes particularly during the post-monsoon season (Sarkar et al., 2018; Bikkina et al., 2019). While model-based approaches face substantial uncertainties (e.g., open fire inventories), direct observational evidence for accurately addressing this pressing issue remains scarce (Kajino et al., 2024; Goyal et al., 2025). Quantifying such impacts is challenging, as disentangling rural stubble burning from local residential biomass combustion is hindered by their overlapping chemical signatures (Zhang et al., 2023), and influences of complex atmospheric transport and aging processes (Joo et al., 2024; Schneider et al., 2024).

Traditional offline analysis using the Aerodyne aerosol mass spectrometer (AMS) has enabled OA source apportionment across time and space (Bozzetti et al., 2017) but is limited by high temperature vaporization (~600 °C) and hard ionization (Canagaratna et al., 2007). The resulting lack of chemical details hinders the ability to resolve OA sources, particularly for complex SOA. New techniques such as extractive electrospray ionization time-of-flight mass spectrometry (EESI-TOF) overcome these limitations by enabling near-molecular characterization with minimal thermal fragmentation. While it has been successful applied in Europe (Qi et al., 2019; Stefenelli et al., 2019; Qi et al., 2020; Casotto et al., 2022), China (Tong et al., 2021; Cui et al., 2024), the deployment in India remains sparse and limited to short period (Kumar et al., 2022; Bhattu et al., 2024).

This study addresses critical knowledge gaps by leveraging EESI-TOF to characterize OA at near-molecular resolution over an entire year in Delhi and Kanpur, two severely polluted IGP cities. By further integrating advanced statistical methods, we have quantified key OA sources, their seasonal dynamics, and associated health impacts. A particular focus is placed on assessing the role of transported agricultural fires emission in urban $PM_{2.5}$ pollution. Our findings offer critical insights to inform targeted air quality management strategies, on local and regional scales.

2. Methods

2.1. Sampling sites, instrumentation, and data processing

A yearlong $PM_{2.5}$ sampling campaign was conducted in the IGP region, known for the elevated $PM_{2.5}$ levels (Fig. S1), with two representative cities, i.e., Delhi and Kanpur, reflecting the regions' pollution seasonality (Fig. S2). The sampling site in Delhi was located at the Indian Institute of Technology Delhi campus, characterized by its urban residential setting and proximity to major roads. The site in Kanpur was located in a suburban environment at the Indian Institute of Technology Kanpur. High-volume samplers (Envirotech Co. Ltd for IITD, Tisch Co. Ltd for IITK) were used at a flow rate of 1.13 m^3 min^{-1} with a sampling schedule including both 12-h intervals during the first three months capturing day/night differences, followed by 24-h intervals during the later period. A total of 275 ambient $PM_{2.5}$ samples were collected from both sites approximately every 4–5 days, covering an entire year as illustrated in Fig. S3. Additionally, five field blank samples were collected by exposing them to routine sampling procedures in the samplers without a flow rate to identify any potential contamination introduced during filter processing. All these samples were carefully stored at −18 °C and used for analysis in this study.

Similar to the offline experimental analysis detailed in Daellenbach et al. (2016), 9 mm filter punches were dissolved in 10 mL of ultra-pure water (Milli-Q®, Merck Millipore, 18.2 MΩ cm at 25 °C, total organic carbon <5 ppb), sonicated at 30 °C for 20 min, vortexed for 1 min, and then filtered through a nylon membrane of 0.45 μm pores (Infochroma AG, HPLC syringe filters YETI). All extracts were then spiked with 150 μL of 200 ppm solution of ^{34}S-labelled ammonium sulphate (Sigma-Aldrich, purity ≥ 90 %), and ^{15}N-labelled ammonium nitrate (Sigma-Aldrich, 98.3 % purity) (Casotto et al., 2022; Bhattu et al., 2024; Cui et al., 2024). These compounds served as carriers to increase the aerosol size for better collection efficiency in the AMS (Williams et al., 2013) and as internal standards for quantification and assessment of instrumental performance. Approximately 4.0 mL extracts were nebulized using synthetic air through an APEX Q nebulizer (Elemental Scientific Inc.), followed by a Nafion® dryer (Perma Pure, MD-070). The aerosol flow then simultaneously passed through LTOF- Aerosol Mass Spectrometer (LTOF-AMS), and EESI-LTOF for the analysis of the water-soluble organic aerosol (WSOA), together with a range of non-refractory inorganic components. The EESI-TOF system with a high mass resolving power of 8 000 at m/z 200 and mass accuracy (≤2 ppm) enables us to obtain the near-molecular information of WSOA and for further source apportionment. The LTOF-AMS data was used for estimating organic matter to organic carbon (OM:OC) ratio of WSOC (Supplementary information (SI) Sec. 3). Additionally, another 3 mL extracts were used to quantify the water-soluble organic carbon (WSOC, measured as non-purgeable organic carbon) using a total organic carbon (TOC) analyzer (Shimadzu, Japan, TOC-L-series).

This study will primarily discuss results derived from EESI-TOF data, which has already been used for offline analysis to characterize organic aerosol at a near-molecular level (Qi et al., 2020; Casotto et al., 2022; Cui et al., 2024). The nebulized aerosol flow was mixed with additional compressed air flow to achieve a tenfold dilution and passed through a charcoal denuder for gaseous contamination removal prior to the EESI inlet. Then, the nebulized aerosol collides with a charged electrospray droplet (100 ppm NaI water solution with pressure regulator set around 150–250 mbar), resulting in the extraction and ionization of the soluble components. The extractive electrospray droplet subsequently traverses a heated capillary manifold (270 °C). This process serves to vaporize the water and generate ions via the Coulomb explosion mechanism, after which the contained compounds are measured by the Api-TOF predominantly as sodium adducts ($[M+Na]^+$). Since the entire process only takes a few microseconds, the potential for thermal decomposition, ionization-induced fragmentation, or matrix effects is minimal, allowing the possibility of analyzing molecular ions. Each sample was measured over an 8-minute period, paired with a Milli-Q water background sample that was also spiked with 3 ppm isotopes for subsequent background subtraction. Data were recorded using TofDAQ software (Tofwerk AG, Thun, Switzerland) at a 1-second acquisition frequency. The raw data were averaged every 20 s and further processed using Tofware software (Tofwerk AG, Thun, Switzerland). The resulting ion clusters of NaI solution, namely $(NaI)\text{-}Na^+$, $(NaI)_2\text{-}Na^+$, $(NaI)_3\text{-}Na^+$, and $(NaI)_4\text{-}Na^+$ were used as mass calibrants. Furthermore, the mass spectrum of all samples, as well as water and field blanks, were averaged over each 8-minute measurement period, during which 20–24 data points were collected

for each sample. Ion filtering was implemented to remove meaningless ions, leaving 955 ions for the final matrix input in PMF analysis. The processed total ion intensities correlated well with AMS-measured WSOA (R = 0.95), as shown in Fig. S5, demonstrating the reliability of the dataset. Additionally, to avoid mixing day/night samples and 24-h samples skewing the PMF results, all 12-h samples for the same day were pre-averaged, resulting in a total of 224 daily samples. More details of the data treatment can be found in SI Sec. 3.

2.2. Additional measurements

In addition, online $PM_{2.5}$ concentrations paired with the sampling sites were retrieved from the Central Pollution Control Board in India (https://cpcb.nic.in/, last accessed on May 9, 2025). Other chemical analyses conducted included organic carbon (OC), elemental carbon (EC), organic acids, water-soluble ions, trace metals, and radiocarbon (^{14}C), with details provided in SI Sec. 6.

2.3. Source apportionment

Source apportionment was first conducted based on the WSOA near-molecular composition. The contributions of those identified aerosol types to total OA was then quantified and corrected using their empirically derived water solubility via a multilinear regression approach. Additionally, contributions from water-insoluble OA linked to liquid fossil fuel combustion were estimated independently. The complete workflow from Sec. 2.1–Sec. 2.3 is outlined in Fig. S4.

2.3.1. Positive matrix factorization analysis

WSOA source apportionment was performed via positive matrix factorization algorithm (PMF) implemented in the multilinear engine-2 (ME-2) solver (Paatero and Tapper, 1994), controlled by the frontend Source Finder (SoFi, Datalystica) (Canonaco et al., 2013, 2021). PMF assumes that variations in the chemical composition of WSOA in a dataset can be represented as the linear product of two matrices plus residues, as in Eq. (1):

$$X = GF + E \tag{1}$$

where X represents the sample matrix of WSOA composition from EESI-TOF which included all samples' mass spectrum with 955 individual fitted ions (m/z 100–360).

The corresponding error matrix was calculated as the standard error of the mean after removing auto-correlation effect, as described elsewhere (Zięba and Ramza, 2011) detailed in SI Sec. 3. F represents the factor profiles (i.e., chemical fingerprint of WSOA sources) for the user-defined number of factors, G represents the concentration time series of those factors/ WSOA sources, and E represents the model residual. In this study, we also make use of the ability of ME-2 to use a priori information on the factor profiles with the so-called a-value approach:

$$f_j^k = (1 \pm a) \bullet f_j^{k,ref} \tag{2}$$

where $f_j^k, f_j^{k,ref}$ represent the loading of species j in resulting factor k and its constrained value in the reference, respectively. $a \in [0, 1]$ is a tolerated relative deviation from the anchor.

Through exploratory PMF runs, we found a factor related to biogenic SOA with a reproducible time series, yet its chemical composition was frequently mixed with other OA types. We also found that several factors strongly associated with biomass burning, while their contributions varied significantly across solutions because of the high variability of the ion $C_6H_{10}O_5$, representing the most important BBOA marker levoglucosan and other anhydrosugars. By exploring PMF solutions ranging from 5 to 20 factors with the same inputs, we observed that some factors displayed clearer and more stable chemical features. Thus, we identified and extracted a biogenic secondary OA factor from a 17-factor solution, and a fresh biomass burning OA factor from a 9-factor solution (profile shown in Figs. S10 and S11 with details in SI Sec. 3). We then used these two factor profiles as prior information with tolerance relative deviation set of 20 % ($a = 0.2$). Finally, the 7-factor solution with 2 constrained factors was found to be optimal. The uncertainty associated with PMF modeling was evaluated by a bootstrapping analysis of 200 runs, i.e., resampling the PMF input in the space–time dimension (Daellenbach et al., 2017). In each bootstrapping run, the factors were sorted according to a reference base case. The final WSOA source contributions were derived by averaging all PMF bootstrapping runs (Hemann et al., 2009), following a selection process based on the criterial detailed in SI Sec. 4. The uncertainties in the derived factor profiles and time series can be seen in Figs. S25 and S26.

2.3.2. Quantification of OA sources

Given the challenge of the insoluble fraction not being measured via filtered water extracts, we adopted an indirect statistical approach to estimate the sources of OA. This involves assuming that 1) all OA types are represented by the WSOA sources besides hydrocarbon-like organic aerosol related to liquid fossil fuel combustion (HOA), 2) each OA type has a constant water-solubility, i.e., WSOC:OC ratio, that we determine via a framework based on multilinear regression (MLR). We established the MLR model via Pystan, a Python interface for the Bayesian model framework (Carpenter et al., 2017). This advanced approach, which treats modelled outcomes as probabilistic rather than deterministic, enhances robustness and allows for the application of constraints preserving physical validity. The approach unfolds in four steps:

Step 1: Set measured WSOC (μg m^{-3}) as the outcome and PMF-derived WSOA types (EESI-TOF signals) as predictors. The aim is to derive the response factor (RF) for each source, scaling EESI-TOF signals to atmospheric WSOC concentrations, expressed as:

$$C_{WSOC,i}\ N(\sum_k RF_k \bullet S_k, \sigma^2_{C_{WSOC,i}}) \tag{3}$$

where $C_{wsoc,i}$ represents the WSOC concentration for sample i, N indicates the normal distribution, S_k is the time series of EESI-TOF signal for source k, RF_k is the response factor for source k, all set with positive constrains, and $\sigma^2_{C_{WSOC,i}}$ represents the variance, accounting for the residual error in the model, set as 10 % of $C_{wsoc,i}$.

Step 2: Set WSOA, calculated by WSOC multiplied with the OM:OC ratios from AMS measurements, as outcome ($C_{WSOA} = C_{WSOC} \bullet OM:OC_{AMS}$) and the EESI-TOF based WSOC source time series derived from step 1 (for source k, $C_k = RF_k \bullet S_k$, in units of μg m^{-3}) as predictors. Similarly, we aim to derive the source-specific OM:OC ratios ($OM:OC_k$, with constrain larger than 1), expressed as:

$$C_{WSOA,i}\ N(\sum_k OM:OC_k \bullet C_{k,i}, \sigma^2_{C_{WSOA,i}}) \tag{4}$$

where $C_{wsoA,i}$ represents the WSOA concentration for sample i, and $\sigma^2_{C_{WSOA,i}}$ as the fitting residual was also set to 10 % of this concentration.

Step 3: Set OC as outcome once accounted for the contribution of hydrocarbon-like organic carbon (HOC), i.e., $OC - HOC$. We assume that all major OC sources can be represented by the resolved WSOA types. Using the same predictor C_k as in step 2, the goal is to derive the source-specific recovery coefficient (RC_k for each WSOA type k, constrained to values greater than 1), which represents the inverse of the OA source's water-solubility expressed as:

$$OC_i - HOC_i\ N(\sum_k RC_k \bullet C_{k,i}, \sigma^2_{OC_i - HOC_i}) \tag{5}$$

where $OC_i - HOC_i$ represents the concentration of $OC - HOC$ for sample i, and $\sigma^2_{OC_i - HOC_i}$ as the fitting residual was also set to 10 % of this concentration. Note that the HOC, being largely water insoluble, could not be directly measured using WSOA extracts. Instead, it was estimated

through a newly developed statistical approach, which decomposed EC into contributions from non-fossil fuel and fossil fuel emissions (details as SI Sec. 7). The resulting uncertainty in the estimated HOC ranged from 8 % to 13 % across sampling days.

Step 4: The reconstructed OA can then be represented as the sum of each OA types' contribution to OC (from Step 3), multiplied by their organic mass-to-organic-carbon ratios (OM/OC) (from Step 2, assuming they are the same for WSOA and OA of a source) and HOC times with OM/OC of 1.21 as per Mohr et al. (2012).

The resulting parameters with associated uncertainties are presented in Table S4. The final scaling factor, accounting for instrument response, water solubility, and OM:OC, exhibited relative uncertainties ranging from 13 % to 42 % across OA factors. Further analysis using 1000 bootstrap samplings, combined with uncertainties from PMF results, showed an uncertainty in the factor contribution to OA annually (Fig. S27) ranged from 0.27 μg m^{-3} to 2.02 μg m^{-3} in Delhi, 0.35 μg m^{-3} to 1.56 μg m^{-3} in Kanpur. Importantly, the ranking of relative contributions of all factors (Fig. S28) was not affected by these uncertainties, demonstrating the robustness and reliability of the results.

2.4. FLEXPART model

A Lagrangian particle dispersion model, Flexible Particle Dispersion Model (FLEXPART) version 10.4, was applied to analyze the air mass origins over the sampling campaign period (Pisso et al., 2019). Meteorological data driving the FLEXPART model were derived from NCEP FNL operational model (https://rda.ucar.edu/datasets/ds083-2/, last accessed on May 9, 2025) with a 6-h interval and 1° × 1° resolution. Three-day backward runs simulated the release of 5 × 10^3 air parcels every hour from both receptor points during the sampling year at 100 m above ground level, with a time step of 180 s. The retroplumes, i.e., potential emission sensitivity (PES) in units of s m^3 kg^{-1}, was calculated as the accumulated residence time of particles in each output grid cell divided by air density in 0.1° × 0.1° resolution for every hour to depict the air mass transport pathways (de Foy et al., 2015). The simulation domain covers all of India and surrounding regions (Fig. S14).

2.5. Health impact assessment

By leveraging near-molecular-level information for improved source identification, we can further estimate the associated health impacts, enabling the development of health-oriented control strategies. Here, we estimated the impact of short-term exposure to PM on mortality (i.e. acute effects) following the non-linear exposure–response model described in Ye et al. (2022). In brief, the mortality burden AD_i attributable to a $PM_{2.5}$ increase ΔX_i for day i can be expressed as:

$$AD_i = D_i \bullet (RR_i - 1)/RR_i \quad (6)$$

$$RR_i = \exp(\beta \bullet \Delta X_i) \quad (7)$$

where D_i represents the daily number of the all-cause death specific region on day i. We assumed a log-linear relationship between the relative risk of mortality (RR_i) and the incremental $PM_{2.5}$ concentration ΔX_i on day i. β denotes the relative risk associated with a 10 μg m^{-3} increase of $PM_{2.5}$, sourced from recent epidemiological studies. Recent studies have demonstrated there is no established $PM_{2.5}$ threshold with no exposure risk (Liu et al., 2019; Yu et al., 2024), ΔX_i was calculated with the baseline set as zero. In absence of daily death counts data for Delhi and Kanpur, we estimated the fractions of the mortality burden attributable to the short-term $PM_{2.5}$ exposure (AD_i/D_i) for each sampling day i. Further, we estimated the contribution of individual OA sources to the relative risk (RR) by using their respective concentration as ΔX to represent associated incremental $PM_{2.5}$. To validate this approach, we summed the AD_i/D_i from all individual OA sources along with the remaining $PM_{2.5}$ mass, assuming a uniform β across all components. The summed mortality burden closely matched that calculated from total $PM_{2.5}$ (within 5 % difference in both cities). Additionally, the registered death data (monthly for Delhi, yearly for Kanpur) were obtained from the official civil registration system (https://dc.crsorgi.gov, last accessed on May 9, 2025) to estimate the number of individuals affected.

3. Results and discussion

3.1. Major chemical components in $PM_{2.5}$ pollution

The average $PM_{2.5}$ concentration for the year 2018 in both Delhi (84 μg m^{-3}) and Kanpur (73 μg m^{-3}) exceeded the WHO recommended limit by more than a factor of 10. Similar to other cities in the IGP region, such as Faridabad and Lucknow, Delhi and Kanpur also showed exceedingly high pollution levels, and notably higher levels observed in cities in South India (Saini and Sharma, 2020; Singh et al., 2021). $PM_{2.5}$ also exhibited strong seasonal variability, with extreme pollution in winter and post-monsoon seasons, when daily levels exceed 200 μg m^{-3} in both cities (Fig. 1). Meanwhile, $PM_{2.5}$ concentrations were lowest during the monsoon, partly due to wet scavenging, since it could account for ~3/4 of the annual rainfall (seasonal meteorological parameters comparison in Table S3) (Deshpande et al., 2012).

Throughout the year, OA constituted a significant portion of $PM_{2.5}$, comprising 46 ± 11 % in Delhi and 49 ± 8 % in Kanpur, acting as the primary pollution driver in both cities, mirroring results from many other cities, e.g., Patna, Varanasi, within the region (Devi et al., 2020; Tobler et al., 2020). This dominance of OA was particularly pronounced during the post-monsoon season, when it accounted for 58 ± 8 % in Delhi and 60 ± 4 % in Kanpur. In addition to OA, major inorganic ions (SO_4^{2-}, NO_3^-, Cl^-, NH_4^+) collectively contributed approximately 30 % to the overall $PM_{2.5}$ mass throughout the year in both cities. The combined concentration of these inorganic ions was notably higher during the winter season, reaching 45.7 μg/m^3 in Delhi and 37.7 μg/m^3 in Kanpur. Organic carbon-to-elemental carbon ratios (OC/EC) were highly dependent on fuel types, combustion conditions, and atmospheric aging processes. The lower OC/EC ratios in Delhi (4.8 ± 2.8) compared to Kanpur (5.8 ± 3.4) suggested a higher contribution from fossil fuel emissions (Wu et al., 2018) and a larger contribution of fresh emissions. Moreover, OC/EC showed similar trends to the OA fraction's, peaking during the post-monsoon season, with averages of 8.7 ± 2.6 in Delhi and 9.11 ± 4.76 in Kanpur. These observations aligned with previous studies in the IGP, emphasizing the more pronounced impacts from biomass burning, enhanced by large-scale crop residue burning after the rice harvest (Srinivas and Sarin, 2014; Bikkina et al., 2019). Such variations in source mixture across seasons and locations further underscore the necessity of detailed source identification for effective mitigation.

3.2. Organic aerosol sources

Near-molecular levels of WSOA composition, further discussed in SI Sec. 8.1, enabled the identification of seven distinct major OA types. Four of these sources were linked to biomass burning: fresh biomass burning OA (F-BBOA), aged biomass burning OA (A-BBOA), nitrogen-containing OA (NOA) associated with primary biomass burning emissions, and agricultural waste burning OA (AgrOA) attributed to transported rural stubble burning. Additionally, two urban-source OA types were identified alongside the estimated hydrocarbon-like OA (HOA, detailed in SI Sec. 6) derived from traffic exhaust emissions. These include a winter-specific urban OA (DIOA) prevalent in Delhi during the colder months, and a mixed urban OA (UOA) influenced by both cooking and traffic activities. Lastly, a biogenic secondary OA (BSOA) was identified, formed through the oxidation of natural volatile organic compounds (BVOCs). The near-molecular composition (Fig. 2), seasonality (Fig. 3) and the underlying impacts from specific emissions, transformations, and transportation, will be discussed in detail in this section. Both F-BBOA and A-BBOA were dominated by $C_6H_{10}O_5$ (likely

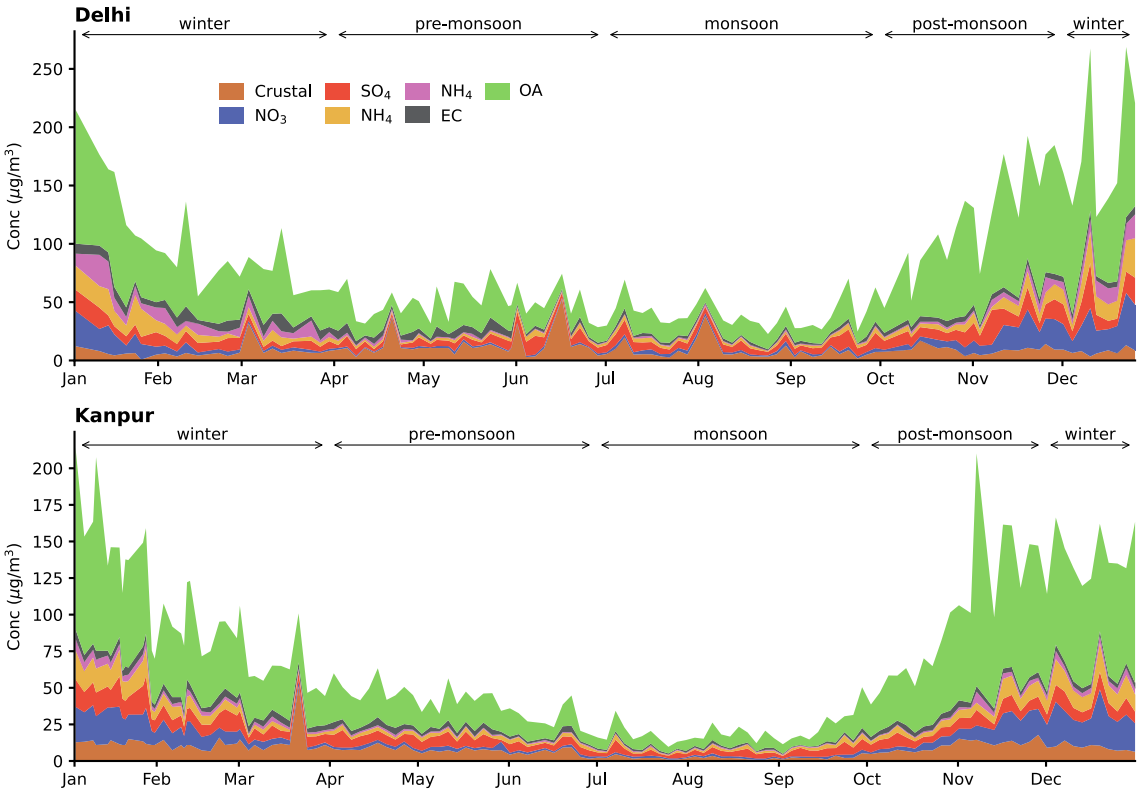

Fig. 1. The time series of major $PM_{2.5}$ chemical components in Delhi and Kanpur in 2018. The seasonal divisions, i.e., winter (January, February, March, December), pre-monsoon (April-June), monsoon (July-September), and post-monsoon (October-November) are indicated by black arrows.

anhydrous sugars, e.g., levoglucosan) and $C_8H_{12}O_6$ (likely a derivative of syringol), common tracers of biomass burning as mentioned earlier. F-BBOA accounted for 42 % of the total ion intensity of $C_6H_{10}O_5$, while A-BBOA contributed less (20 %). This is consistent with levoglucosan degrading during atmospheric aging (Yazdani et al., 2023) and is in line with other research that also resolved fresh and aged BBOA (Qi et al., 2019; Kumar et al., 2022). Moreover, F-BBOA displayed higher fractions of large *m/z* CHO compounds with typical formulas of $C_{14\text{-}17}H_{16\text{-}20}O_{4\text{-}5}$ including abundant compounds such as $C_{17}H_{20}O_4$, $C_{17}H_{20}O_5$ and $C_{16}H_{18}O_6$ that were also observed in fresh biomass burning plumes or burning experiments (Brege et al., 2018, 2021; Fleming et al., 2020). In contrast, A-BBOA was characterized by a higher fraction of CHNO compounds than F-BBOA (33 % vs 22 %). These ions mainly contained 9–11 carbon atoms (Fig. 2 and Fig. S23), with prominent ions detected as $C_9H_{11}NO_2$-$(CH_2)_n$-Na^+ (e.g., $C_9H_{11}NO_2$, $C_{10}H_{13}NO_2$, $C_{11}H_{15}NO_2$), likely nitro-aromatic compounds secondarily formed from phenolic precursors such as phenols and cresols emitted during biomass burning (Bertrand et al., 2018; Niu et al., 2020; Li et al., 2024). The time series of F-BBOA and A-BBOA were generally similar, with higher concentrations observed during colder months (Dec-Feb, temperature profiles in Fig. S24). Such wintertime concentration enhancements were likely caused by a combination of increased residential heating demand and meteorological conditions that hindered ventilation (Table S3), such as weak surface winds, minimal rainfall, and low planetary boundary layer, which are common in North India during winter (Pawar and Sinha, 2022; Garsa et al., 2023). A correlation matrix combining PMF factors with selected auxiliary measurements as potential source tracers can be seen in Fig. S29. F-BBOA showed the highest correlation with levoglucosan from auxiliary data (R = 0.95). The differences in the time series between the cities indicated that F-BBOA was more strongly associated with fresh local emissions. Meanwhile, A-BBOA correlated less with levoglucosan but slightly better with NO_3^- and NH_4^+ (R = 0.78 and 0.76, respectively), consistent with aged emissions. When nighttime temperature sharply decreased and emissions intensified, OA could be substantially enhanced by the condensation of primary biomass burning vapours (Mishra et al., 2023). Such formation in winter, driven by seasonal meteorological changes, might explain the correlation between A-BBOA and NH_4^+, NO_3^-, influenced by similar thermodynamics.

The mass spectrum of Nitrogen-containing OA (NOA) featured a pronounced presence of CHN ions (accounting for 17 % in the profile), which was 2–8 times that of other OA types. Compounds with 2 nitrogen atoms represented nearly 90 % of the signal within the CHN group with major homoologous series of two types, i.e., $C_7H_{12}N_2$-$(CH_2)_n$ and $C_8H_8N_2$-$(CH_2)_n$. The former is likely a derivative of imidazole, characterized by a heterocyclic core with two nitrogen atoms and an appended alkyl chain, while the latter could be azaindole derivatives with the core structure of a fused two-ring system, which includes a six-membered pyridine ring and a five-membered pyrrole ring. The presence of 2-N containing species has been noted in abundance from cow dung and brushwood burning cookstoves in India (Fleming et al., 2018) and straw residue burning in China (Lin et al., 2012; Wang et al., 2017). These species are most likely to originate from N-heterocyclic alkaloid compounds produced from biological sources such as plants and animals (Laskin et al., 2009).

The time series of NOA (Fig. 3) demonstrated a good correlation with levoglucosan (R = 0.75) with higher concentrations during the cold months. We observed a clear nighttime increase in 2-N containing species, in contrast to the CHO and CHNO groups, with some increasing more than ten times (Fig. S22 details discussed in SI Sec. 8.1). Such differences might indicate intensified emissions during nighttime or could result from secondary formation processes, e.g. imidazole-like compounds may also result from aqueous reactions of α-dicarbonyls with ammonium or amine (Li et al., 2023b; Gan et al., 2024) with potential products like $C_7H_{12}N_2$ (De Haan et al., 2011) observed in NOA. However, no correlation was observed between these compounds and relative humidity or the liquid water content modelled with thermodynamic equilibrium model ISORROPIA II (Fig. S30) (Fountoukis and Nenes, 2007). Furthermore, phenolic SOA tracers such as $C_8H_6O_5$,

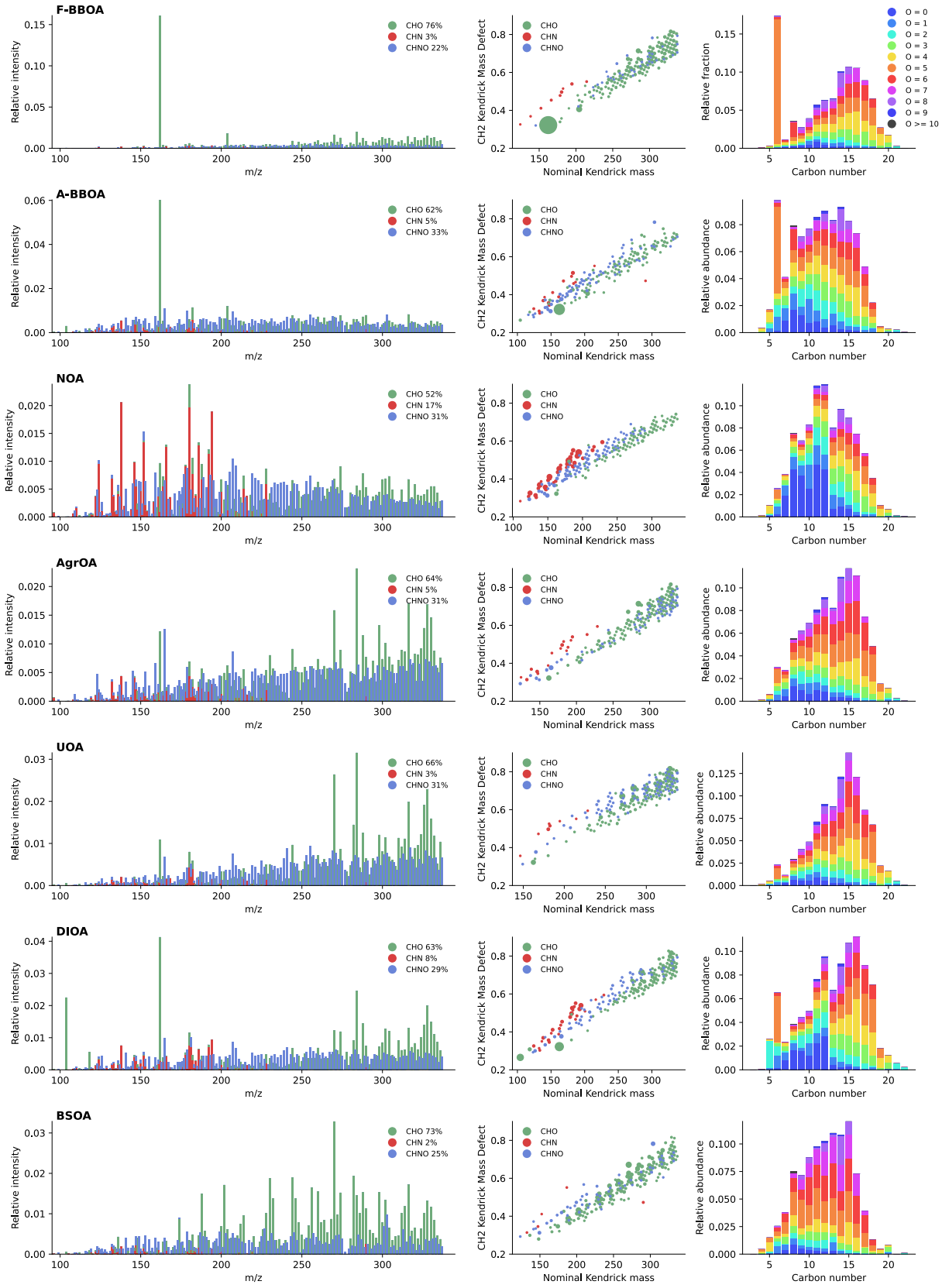

Fig. 2. The molecular chemical composition of OA sources (neutral compounds) based on EESI-TOF analyses depicted in the unit mass spectrum (left), CH_2-Kendrick mass defect plot for the most abundant 200 ions, with the size scaled by the ion intensity (central) and carbon number distribution color-coded by oxygen number (right).

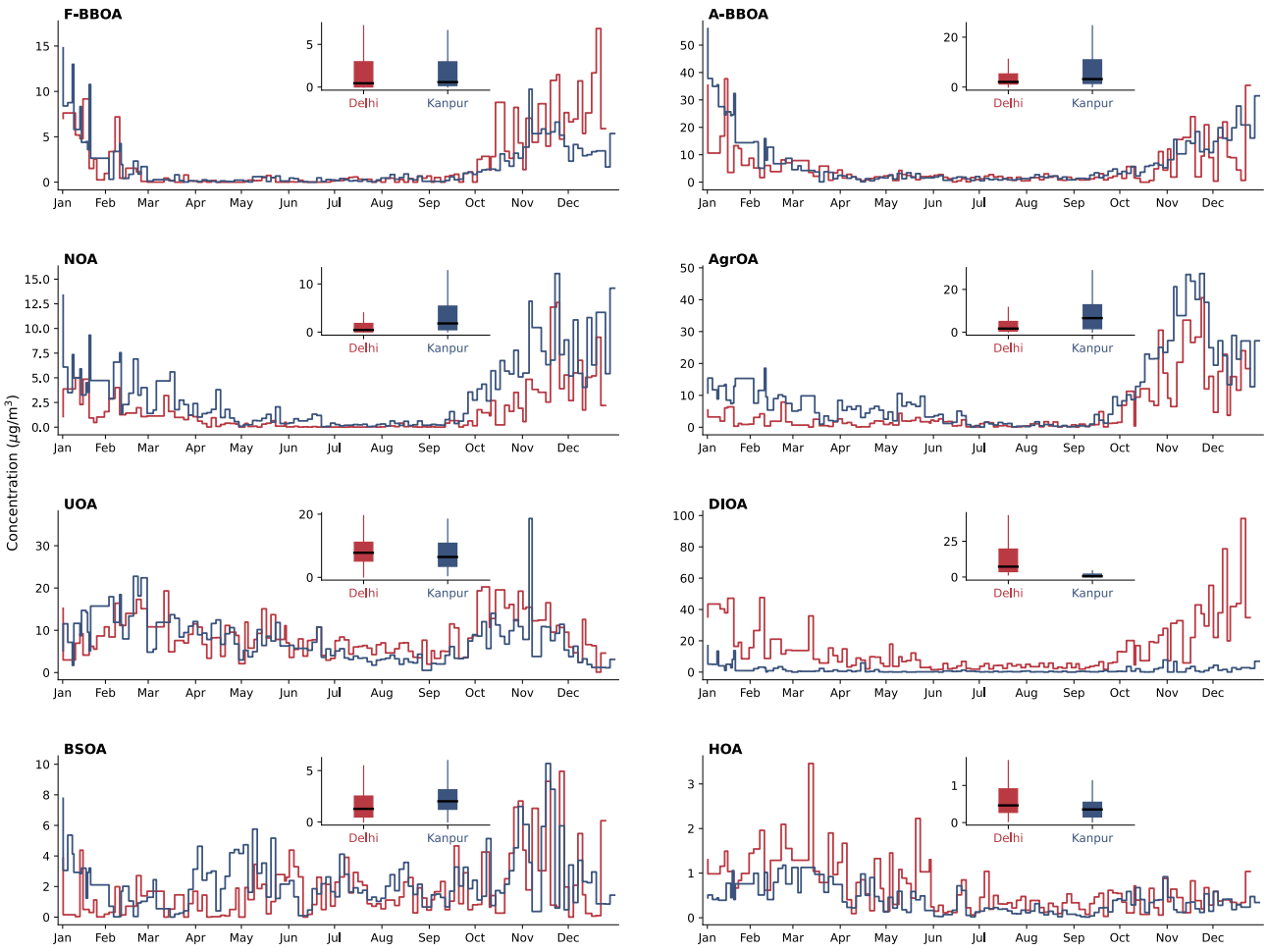

Fig. 3. Time series of concentrations for all OA types in Delhi and Kanpur with box plots summarizing their annual variations. The bold lines within the boxes indicate mean values, the boxes represent the interquartile range (IQR) between the first (Q1) and third (Q3) quartiles, and whiskers extend to Q1 − 1.5 × IQR and Q3 + 1.5 × IQR.

$C_8H_{10}O_6$, known to form through aqueous-phase oxidation of phenols from biomass burning (Yu et al., 2016; Xiao et al., 2022), did not show a clear nighttime increase. This suggests that nocturnal aqueous-phase processing is not a contributor to NOA in our case. Collectively, all observations point toward intensified nighttime primary emissions rather than nocturnal secondary formation as the major contributor of NOA. Thus, the use of biomass fuel for household heating could be a significant OA source (Navinya et al., 2023), with maximum contributions exceeding 10 μg m^{-3} in both cities. This unique factor, possibly mixed into the cold-season primary OA factor in Bhattu et al. (2024), has not been identified in similar studies in Europe or China, while its significance in India could not be overlooked. Since traditional biomass fuels remain a primary energy source in rural India (Mishra et al., 2024), the higher NOA levels in Kanpur (average of 3.4 μg m^{-3}) compared to Delhi (average of 1.5 μg m^{-3}) suggest a more extensive use of such fuels in rural Uttar Pradesh.

While F-BBOA, A-BBOA, and NOA were most probably related to residential biomass burning, an additional BBOA type was successfully identified, representing the impacts of rural agricultural burning (Agricultural fire OA − AgrOA), evidenced primarily by its unique time series. The impact of such agricultural fires could not be resolved in previous studies. Specifically, AgrOA concentration peaks occurred for both cities from late October to mid-November with maximum contributions to OA exceeding 40 μg m^{-3}. This aligns with the timing of the widespread practice of burning rice straw residues after the harvest in North India (Sarkar et al., 2018; Bikkina et al., 2019). The integration of Lagrangian retroplumes and fire spot maps (Fig. 4, Fig. S31) further supported the link between AgrOA and transported emissions from agricultural waste burning. Open fires were widely distributed across the Indian subcontinent with three intensive periods throughout the year (Fig. S32). These include March to April, mainly in central and northeast India due to forest fires; May, primarily in northwest India from wheat residue burning; October to November, also mainly in northwest India, from rice/paddy residue burning. Interestingly, only the third burning period showed the clearest impacts, as prevailing northwesterly winds transported pollution plumes primarily from Punjab, where intense fires occurred. In addition, the unique topography of the IGP, bounded by the Himalayas to the north and the Vindhya range to the south, could restrict pollutant dispersion transported from the upwind region, effectively trapping them within the densely populated basin until exited over the Bay of Bengal (Fig. S33). The resulting OA contribution averaged 39.0 μg m^{-3} in Kanpur and 21.6 μg m^{-3} in Delhi, both located downstream during the post-monsoon period. This pattern contrasted with earlier fire periods in March-April (forest fires) and May (wheat straw fires) which can be explained by different meteorological conditions. In the latter two periods, the intense fire activities did not coincide with the dominant airmass transport pathways directed toward the two cities and were accompanied by stronger dispersion conditions during the pre-monsoon (Table S3), resulting in minimal impact. Fig. S34. Comparing the potential source regions and air mass trajectories of these three periods, further elucidated that post-monsoon fires in northwest India coincide with rapidly descending air masses near the

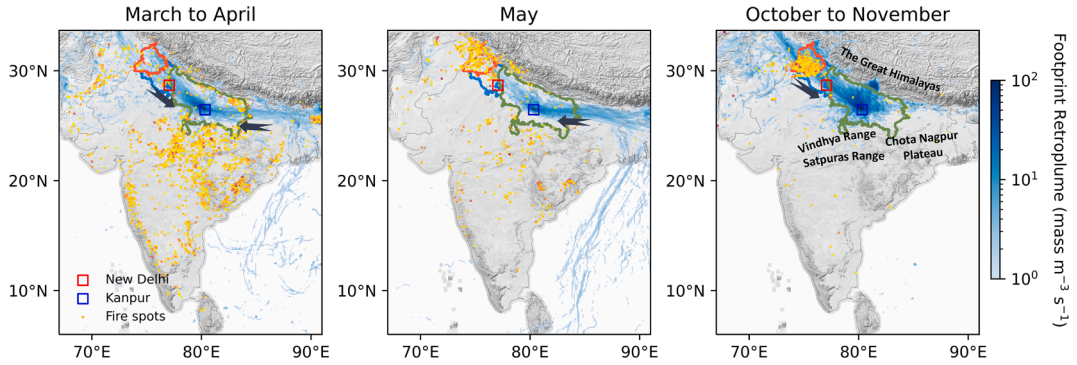

Fig. 4. Geographical origin of air masses arriving in Kanpur displayed as the footprint layer of accumulated 72-hour FLEXPART backward retroplumes during three intensive fire periods, overlaid by the Visible Infrared Imaging Radiometer Suite active fires (https://eogdata.mines.edu/products/vnf/, last accessed on May 9, 2025) and topographic shading for terrain visualization (http://www.naturalearthdata.com, last accessed on May 9, 2025). Arrows indicate predominant air mass transport direction. Three Indian states, i.e., Punjab (outlined in red), Haryana (outlined in blue), and Uttar Pradesh (outlined in green) are depicted. Major mountain ranges, such as the Great Himalayas and the Vindhya Range, which confine air masses within the Indo-Gangetic Plain (IGP), are also annotated. (For interpretation of the references to color in this figure legend, the reader is referred to the web version of this article.)

surface, facilitating the transport towards IGP. This finding, consistent with previous studies (Kaskaoutis et al., 2014; Ravindra et al., 2021; Lan et al., 2022; Montes et al., 2022), highlights that the rice stubble burning exerted a greater impact than wheat in the region, related to favorable meteorology. Additionally, the uncertainty analysis validated the quantification, with the annual contribution to OA estimated within a relatively narrow range of 12.5 ± 2.1 % and 28.3 ± 3.6 % (Figs. S27 and S28).

AgrOA's chemical information further confirmed its association with aged biomass burning smoke. AgrOA was characterized by the highest fraction of $C_9H_{11}NO_2$ (0.9 %) as well as other CHNO ions such as $C_9H_{5\text{-}9}NO_{4\text{-}6}$, $C_{10}H_{7\text{-}9}NO_{4\text{-}5}$, $C_{11}H_{11}NO_5$, in which AgrOA accounted for more than 75 % of their variances. These CHNO compounds are likely nitrophenolic compounds, similar to those mentioned in A-BBOA, but with higher O/C and lower H/C ratios, as well as larger molecular weights, suggesting they could be more oxidized and further functionalized. This is likely due to longer transport and aging times, as the major source region—harvested cropland—was farther from the cities compared to the other BBOA types. Moreover, these CHNO ions, predominantly explained by AgrOA, aligned with findings from Wang et al. (2019), which ascribed nitrophenol-like compounds detected on the Tibetan Plateau to transported biomass burning plumes from the IGP region. In addition, enhanced toxicity of BBOA after atmospheric aging has been reported and is partially attributed to these nitro-phenol-like SOA, as they are strongly associated with ROS production (Wang et al., 2023; Fang et al., 2024). From this perspective, the potential hazards of AgrOA should not be overlooked. Additionally, the levoglucosan content in AgrOA (1 %) was found to be more than 15 times lower than in F-BBOA and 5 times lower than in A-BBOA. Such degradation of the major chemical fingerprint of fresh BBOA aligns with previous works (Hennigan et al., 2010; Zhang et al., 2024). Meanwhile, oxygenated aromatics (e.g., phenol) and heterocyclic compounds (e.g., furan) serve as key precursors that can sustain SOA formation, prolonging the air quality impacts of AgrOA for over a week (Vasilakopoulou et al., 2023; He et al., 2024).

While these biomass burning OA types overall contributed to 35 % of OA in Delhi and 66 % in Kanpur, the influence of other anthropogenic sources accounted for 61 % in Delhi, and 28 % in Kanpur.

Urban mixed OA (UOA) comprised OA components that undergo aging processes from complex urban emissions such as traffic and cooking, similar to OA types previously identified in several cities of North India (Bhattu et al., 2024). Its spectrum showed three prominent ions, $C_{15}H_{26}O_4$, $C_{16}H_{28}O_4$, $C_{18}H_{32}O_5$, and a high abundance of large *m/z* CHO compounds such as $C_{13\text{-}18}H_{20\text{-}32}O_{4\text{-}7}$. Such CHO species can be formed from aliphatic hydrocarbons, abundant in vehicle exhaust, especially from diesel since 80 % of its SOA is produced from long-chain alkanes (≥C15) (Madhu et al., 2023). Moreover, the mentioned compounds could also originate from unsaturated fatty acids, primarily emitted from cooking (Li et al., 2023a). For example, $C_{18}H_{32}O_5$ has been found to be one of the main products from oleic acid ($C_{18}H_{34}O_2$) oxidation by O_3 (Al-Kindi et al., 2016). In comparison to all other OA types, UOA showed stronger correlation with EC and displayed similar seasonal trends, especially in Kanpur (Fig. S35). A spike of UOA in Kanpur was found on November 7th (29.2 μg m^{-3}), coinciding with Diwali festival, when emissions from ritual bonfires, fireworks, incense, and oil lamps may contribute as unique urban sources. Excluding this special day, UOA in Kanpur correlated better with EC (R = 0.67) and Vanadium (R = 0.55), the latter typically emitted from fuel and lubricating oil in tailpipe (Amato et al., 2011; Jawaa et al., 2024), strengthening its link with urban combustion.

Another OA type, termed Delhi industrial OA (DIOA), exhibited substantially higher concentrations in Delhi, especially in winter. The prominent compounds in DIOA shared common features: 1) Concentrations in Delhi were typically fivefold higher than Kanpur, 2) Night-to-day ratios, offering additional insights onto emissions/formation pattern, reached up to 3, higher than those of directly emitted EC, and 3) High correlation with Cl^- (R > 0.6), displaying pronounced seasonality with a tenfold difference between winter and monsoon. Among these ions, the most prominent—accounting for over 90 % of their total intensities in the DIOA factor—were chemically similar compounds with the formulas $C_3H_6N_6$ and $C_4H_8N_8$. These are likely melamine and its derivative, methylene melamine, which are widely used in the manufacture of plastics, laminates, and adhesives (Lütjens et al., 2023). These compounds can be released into the atmosphere during industrial processes involving production, and they as semi-volatile organic compound (SVOC) are more likely to condense into particle phase during colder winter months (Watanabe et al., 2007). Elevated levels of melamine have previously been observed in e-waste dust, largely attributed to emissions from the recycling of printed circuit boards (PCBs) with melamine commonly used as a flame retardant (Li et al., 2022). Given that Delhi is one of the most prominent hubs for informal e-waste recycling, this likely explains the substantially higher levels of those compounds observed in the city (Gangwar et al., 2019; Arya et al., 2021). This explanation was further supported by the strong correlation between those ions and Cl^-, as the extremely high particle-bound Cl^- concentrations reported in Delhi are believed to originate from similar sources, such as waste burning (including plastics) and industrial processing (Tobler et al., 2020; Rai et al., 2020; Cash et al., 2021; Gunthe et al., 2021; Faisal et al., 2022), and its winter increase driven by lower temperature and higher relative humidity (Manchanda et al., 2022).

Due to their low water-solubility, the concentration of fresh OA emissions from liquid fossil fuels (Hydrocarbon-like OA, HOA) was inferred via a tracer approach based on elemental carbon and levoglucosan validated by ^{14}C analysis of EC (details in SI Sec. 6). The estimated HOA concentrations were substantially higher in Delhi (0.65 ± 0.57 μg m^{-3}) compared to Kanpur (0.40 ± 0.30 μg m^{-3}), as confirmed by a Mann-Whitney *U* test ($P < 0.05$). This difference, which aligned with Lakra et al, (2024) comparing HOA in Delhi, Kanpur and Lucknow, was due to higher density of Delhi's vehicles. The time series of HOA in both cities displayed relatively consistent levels through the year, indicating steady local emissions. A similar factor in Bhattu et al. (2024) attributing to fresh traffic emissions, was found to be one of the dominant contributors to oxidative potential (OP). Therefore, the associated potential health risks warrant further attention, particularly in Delhi.

Finally, biogenic SOA (BSOA, 5 % of OA in Delhi, 7 % of OA in Kanpur) was characterized by a large contribution of CHO compounds with a high degree of oxygenation such as $C_4H_6O_5$, $C_5H_{12}O_4$, $C_8H_{12}O_5$, $C_9H_{14}O_5$, $C_9H_{16}O_5$, $C_{10}H_{16}O_6$, $C_{11}H_{16}O_6$, $C_{15}H_{26}O_4$. Similar BSOA profiles with many matching formulae were found in e.g. Delhi (Kumar et al., 2022) and Zurich, Switzerland (Stefenelli et al., 2019; Qi et al., 2020), implying the oxidation of common biogenic precursors, e.g., isoprene (C_5H_8), monoterpenes ($C_{10}H_{16}$) and sesquiterpene ($C_{15}H_{24}$). For example, $C_{15}H_{26}O_4$ as the most abundant ion (accounting for 2 % in BSOA) could result from oxidation of sesquiterpene. $C_4H_6O_5$ and $C_5H_{12}O_4$, largely explained by BSOA, could be isoprene SOA products (Nguyen et al., 2010; Chen et al., 2020). Additionally, the time series of BSOA correlated well with independently measured biogenic SOA marker molecules: 4-Oxoheptanoic acid ($C_7H_{12}O_3$, R = 0.61) and tartaric acid ($C_4H_6O_6$, R = 0.67) (Fig. S36). Notably, 4-Oxoheptanoic acid has been identified in α-pinene SOA (Cook et al., 2017) and tartaric acid can be formed through isoprene photooxidation (Fu et al., 2008), both of which corroborate our findings. However, other biogenic SOA markers such as pinic acid ($C_9H_{14}O_4$) and 3-MBTCA ($C_8H_{12}O_6$) were not compared because their levels in the auxiliary data were too low for quantifcation, implying concentrations much lower than what measured in Europe during summer (Glojek et al., 2024). In contrast to other OA types, BSOA exhibited relatively minor concentration differences between the colder and monsoon seasons. The substantial increase in emissions of precursors from July to August (Fig. S37) coupled with intense photooxidation (average temperature above 30 °C) could lead to higher BSOA production, offsetting the decline caused by monsoon heavy rainfall (Table S3).

3.3. Contributions of OA sources across seasons

While OA remained a major $PM_{2.5}$ component across seasons in both cities, the primary sources varied in their contributions, as seen in Fig. 5. Annual factor contributions (Fig. S38) showed that DIOA contributed the most in Delhi (14.7 μg m^{-3}, 36 % of OA), followed by UOA at 22 %, A-BBOA and AgrOA at 13 % each, with all other OA types contributing less than 10 % each. In Kanpur, although AgrOA showed large seasonal variation, it still averaged annually as the most important OA contributor (10.0 μg m^{-3}, 28 %), followed closely by A-BBOA and UOA at 22 % each. Clearly, OA types related to local emissions of traffic and industry, or cooking (HOA + DIOA + UOA) were more prevalent in Delhi, comprising 60 % of OA, compared to 25 % in Kanpur. In contrast, biomass burning factors (F-BBOA, A-BBOA, NOA, AgrOA) were dominant in Kanpur (23.1 μg m^3, 65 % of OA). Yet, their importance in Delhi was still considerable at 34 % with peak levels reaching 75 μg m^{-3}.

During the pre-monsoon and monsoon periods, the disparity in pollution levels between Delhi and Kanpur was more pronounced with $PM_{2.5}$ levels of 41.3 μg m^3 versus 20.6 μg m^3 during the monsoon, and 54 μg m^3 versus 42.6 μg m^3 during the pre-monsoon. This notable difference, compared to polluted seasons (post-monsoon, winter), was partly due to higher contributions of UOA and DIOA in Delhi, which made up more than 60 % of OA, highlighting the need to alleviate local emissions within and surrounding the city. In Kanpur, UOA was the largest OA contributor during the pre-monsoon (40 %) and monsoon (35 %), while emissions from biomass burning also played a substantial role (together accounting for ~40 %). Notably, AgrOA in Kanpur during

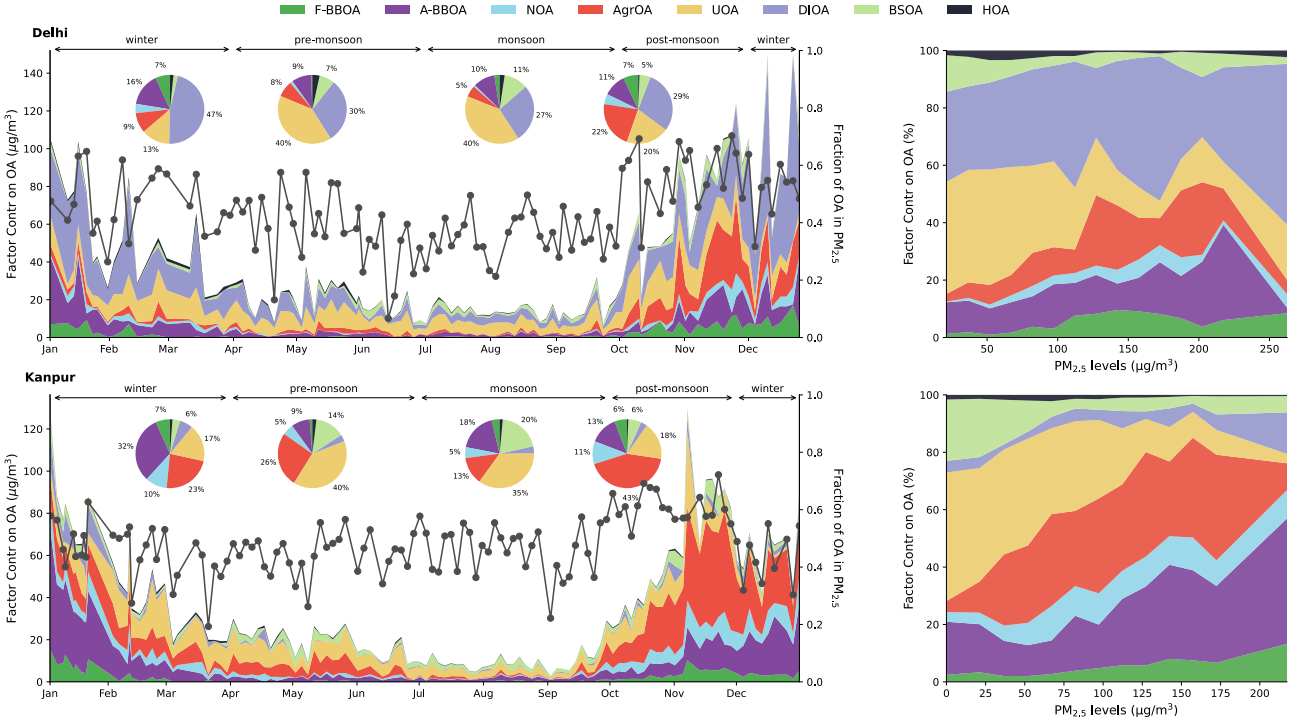

Fig. 5. Stacked concentration time series of all OA types and the fraction of OA to $PM_{2.5}$ in Delhi and Kanpur throughout the year (left) and their corresponding relative contributions to OA as a function of $PM_{2.5}$ levels (right). Seasonal relative contributions are illustrated with pie charts, where the leftmost pie chart represents the winter season (average of January, February, and December).

the pre-monsoon season still accounted for a considerable 26 % of OA, although clearly lower compared to the post-monsoon season, reflecting smaller impact of wheat stubble burning compared to rice stubble burning, as previously discussed.

Severe $PM_{2.5}$ pollution usually occurred during post-monsoon and winter seasons, with winter average levels being higher (134.3 μg m^{-3} in Delhi and 118.1 μg m^{-3} in Kanpur). During winter, OA remained the largest $PM_{2.5}$ component (OA/$PM_{2.5}$ at 40–60 %) in both cities, with elevated contributions from OA associated with local biomass burning (Fig. S39). Specifically, local BBOA (F-BBOA + A-BBOA + NOA) in Kanpur contributed a total of 26.0 μg m^{-3} in winter, representing 48 % of OA, with peak up to 84.2 μg m^{-3}. This likely reflects more intense use of domestic heating using biomass during cold months there. In contrast, local BBOA accounted for only 27 % of OA in Delhi during winter, while DIOA contributed 47 % of OA, averaging 30.5 μg m^{-3}. We believe this substantial increase was driven by gas-particle condensation of volatile compounds emitted/oxidized there, a process that was more pronounced during cold and foggy winter.

As for the post-monsoon season, a marked difference in pollution causes compared to winter was noted, characterized by an increased contribution of OA to $PM_{2.5}$ (OA/$PM_{2.5}$ typically >0.6), mainly driven by AgrOA in both cities. Specifically, the average concentration of AgrOA in Delhi rose to 15.6 μg m^{-3}, representing 22 % of OA. During the intensive burning period from November 16–25 (Fig. S31), AgrOA peak levels were between 26.6 μg m^{-3} and 40.6 μg m^{-3}, accounting for nearly half of OA and serving as the key driver of this prolonged haze episode. In Kanpur, AgrOA contributed almost half of OA, with an average contribution 26.5 μg m^{-3} (43 % of OA). In November, more than 50 % of sampling days experienced AgrOA exceeding 40 μg m^{-3}, accounting for 70 % of OA, underscoring the dominant role of AgrOA in severe episodes pollution there. These findings highlighted that transported and aged OA from rice straw burning in northwest India, particularly Punjab, substantially impacted air quality, triggering haze pollution extending to downstream cities during the post-monsoon season. Such long-distance impacts have also been observed in cities such as Lucknow and Patna, and even extending towards the Tibetan Plateau, China (Wang et al., 2019; Goetz et al., 2022; Saxena et al., 2024). Interestingly, Kanpur, located 600 km downstream of the stubble burning hotspots, appeared to experience an even greater impact than Delhi. This could be related to the different aging times affecting the two cities. Studies have reported more fires in the afternoon compared to the morning in north India (Vadrevu et al., 2011). This is further supported by geostationary satellite images (Fig. S40) which revealed that the stubble fires in Punjab typically began in the late afternoon (~3 PM local time). The backward trajectories on individual days (Fig. S41) show that during this season air masses predominantly originated from the mountainous region, descended rapidly over North Pakistan and Punjab, and moved towards the IGP - guided by surrounding mountains. After picking up emissions from burning fields, the air travelled approximately 12 hs until reaching Delhi, while it took more than 24 hs before reaching Kanpur. Further source region analysis during high AgrOA impact days (Fig. S42) confirmed such travel time differences between the two cities from Punjab. Based on these, AgrOA plumes arriving in Delhi were likely to experience limited aging due to much of the journey occurring overnight, with minimal photochemistry. In contrast, the prolonged journey to Kanpur allowed for more extensive photochemical aging and SOA formation, particularly from precursors like intermediate and semi-volatile organic compounds (He et al., 2024), resulting in higher AgrOA concentrations in Kanpur.

3.4. Implications from source-specific exposure risk

Short-term exposure to the high $PM_{2.5}$ levels in Delhi and Kanpur is expected to have adverse health impacts (Zhao and Wang, 2024). Given AgrOA's regional impacts on severe post-monsoon haze which potentially affects the densely populated IGP, assessing its acute health impacts is particularly critical. Recent studies have shown that wildfire-related $PM_{2.5}$ (including crop residue burning) poses greater health risks compared to $PM_{2.5}$ from non-wildfire sources (Aguilera et al., 2021; Ye et al., 2022). To better assess the specific health impacts, we drew upon global epidemiological studies that encompass highly polluted regions and explicitly account for crop residue burning within wildfire-related $PM_{2.5}$ exposure estimates, thereby enhancing the representativeness and relevance of our assessment. Based on Chen et al. (2021), a relative risk (RR) of 1.021 (95 % CI: 1.018–1.024) was applied for all-cause mortality associated with a 10 μg m^{-3} increase in AgrOA-related $PM_{2.5}$. For comparison, the RR associated with other $PM_{2.5}$ components was set at 1.0068 (95 % CI: 1.0059–1.0077) referencing to Liu et al. (2019). The elevated RR for AgrOA was further supported by Bhowmik et al. (2024b), which indicated the toxicity of $PM_{2.5}$, represented by its OP, was higher during the post-monsoon in Delhi. Additionally, due to the unavailability of daily death data, we assumed the daily death number did not vary throughout the year, as evidenced by the relatively consistent monthly death count in Delhi (Fig. S44). This assumption enabled us to assess the seasonal and yearly averages of the mortality burden fraction attributable to short-term $PM_{2.5}$ exposure.

As illustrated in Fig. 6, the acute mortality associated with $PM_{2.5}$ posed a great environmental health risk in both cities, contributing to a substantial portion of all-cause deaths (average of 6 ± 4 % in Delhi, 6 ± 5 % in Kanpur), with such risk escalating to 20 % during the pollution episodes. This high $PM_{2.5}$-attributable mortality was twice higher than the global average (2 %) and demonstrated consistency with a recent study reporting acute mortality burden across 10 Indian cities (averaging 7.2 %), though lower than reported estimates for chronic impacts (10.4 % of total deaths across India) (India State-Level Disease Burden Initiative Air Pollution Collaborators, 2021; de Bont et al., 2024; Yu et al., 2024). The total contribution of all OA factors (Fig. S43 with more discussion in SI Sec. 8.5), was estimated to account for 47 % of the annual $PM_{2.5}$-attributable mortality in Delhi and 57 % in Kanpur, with the fraction close to 80 % during pollution episodes. This corresponded to over 4000 premature deaths annually in Delhi and more than 600 in Kanpur, assuming relatively consistent daily mortality rates throughout the year.

Specifically, the fraction of deaths attributable to the AgrOA within $PM_{2.5}$-associated burdens was 11 % in Delhi and 27 % in Kanpur on an annual basis. Meanwhile during the post-monsoon season, these fractions increased substantially to 32 % in Delhi and 53 % in Kanpur, ranking as the highest among all OA factors during this period. In terms of attributable deaths, an estimated 1072 deaths in Delhi and 259 deaths in Kanpur were linked to this AgrOA during October to November, corresponding to 5.5 and 9.4 deaths per 100,000 population, respectively. Notably, on highly impacted pollution episodes in Kanpur, far away from AgrOA's main source region, it could account for approximately 10 % of the deaths. Moreover, Ye et al, (2022) found that females and adults aged ≥60 years were more vulnerable to wildfire emissions. Using their respective RR values from literature, AgrOA's contribution to acute $PM_{2.5}$-attributable female mortality during the post-monsoon could reach 46 % in Delhi and 67 % in Kanpur. For older adults, AgrOA's relative risk was 1.43 and 1.28 times higher in Delhi and Kanpur compared to adults younger than 60 years during this period. These figures highlight, that transported rural fire smokes remains a major detrimental factor threatening public health, despite intensive urban emissions. Considering the limitations of existing epidemiological findings and the lack of detailed death data, the current health risk estimation might involve uncertainties related to the use of RR values and other underlying assumptions. A further uncertainty analysis, detailed in SI Sec. 8.5, confirmed the robustness and reliability of the results.

Bhattu et al. (2024) identified local incomplete combustion in North India as the largest contributor to OA and its oxidative potential. Similarly, our results emphasized the importance of local biomass burning, with increased importance in wintertime. These findings collectively

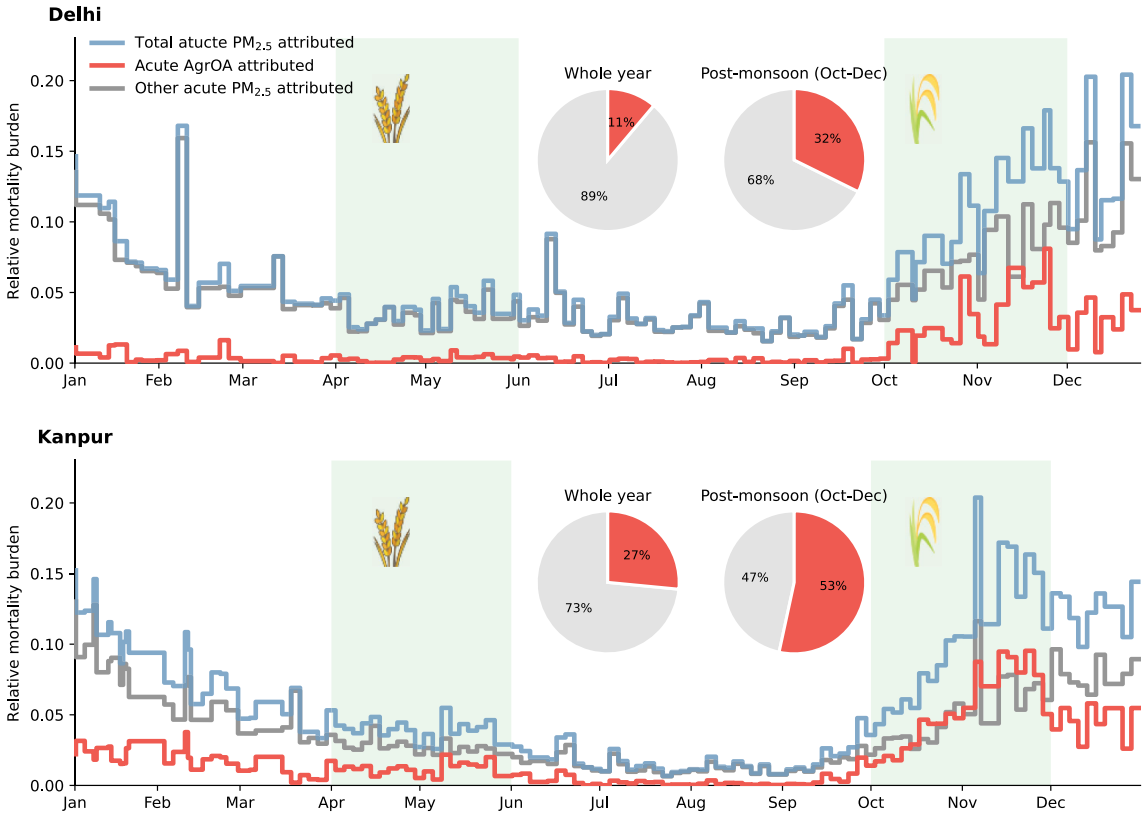

Fig. 6. Time series of attributable burden of acute mortality due to $PM_{2.5}$ exposure and AgrOA exposure in Delhi and Kanpur. Pie charts illustrate the contribution of AgrOA and other $PM_{2.5}$ components to $PM_{2.5}$ related acute mortality. Green shadings highlight the typical harvest periods of wheat (April-May) and rice (Oct-Nov) in North India (image icons extracted from www.flaticon.com). (For interpretation of the references to color in this figure legend, the reader is referred to the web version of this article.)

support the need for policies targeting emission reduction from domestic fuels like wood, cow dung, and rice husk. This can be achieved by promoting the use of improved, cleaner cookstoves with features such as forced draft or less fuel consumption. (Arora et al., 2020). Meanwhile, the transition of informal household fuels to cleaner alternatives, such as Liquefied Petroleum Gas (LPG) and electricity, requires improving energy infrastructure to enhance accessibility and implementing price subsidies to make these options more affordable for low-income communities. (Chowdhury et al., 2019; Sharma and Jain, 2019; Chanchani and Oskarsson, 2021). Furthermore, our year-long observations allowed us to gain more insights for developing targeted policies based on OA sources across the seasons. Specifically, we found the significance of rather local emissions in Delhi during winter on OA pollution (DIOA), which accounted for 20 % of total $PM_{2.5}$-attributable mortality there. To address this, regulatory measures should prioritize controlling emissions from industries, including stricter enforcement of emission standards for factories, and addressing informal sectors such as e-waste recycling, which often operates without appropriate control measures (Gangwar et al., 2019).

More importantly, AgrOA cannot be overlooked due to its considerable contribution to acute mortality burden in both cities, even though relevant pollution events were only during a short period. Mitigation measures should extend beyond cities to regional scales, targeting regions particularly affected by stubble fires like Punjab and Haryana, combining mandatory regulations and incentive-driven approaches. In addition to enforcing a ban on open burning, in-situ management can be promoted through subsided machinery, such as the "Happy Seeder" enabling wheat sowing into harvested rice fields without burning straw (Keil et al., 2021), and by providing incentives for using straw as fertilizer, a practice successfully implemented in China (Bai et al., 2023). Ex-situ management, such as using stubble for livestock fodder or energy production, requires infrastructure development for straw collection/transport and subsidies as incentives (Dutta et al., 2022). Considering that these fires coincide with meteorological conditions that trap smoke and transport it downstream to populated regions (Liu et al., 2022), promoting crop diversification, or transitioning to short-duration, low-straw-generating rice varieties in Northwest India could also facilitate mitigating such pollution (Kant et al., 2022; Mukherjee et al., 2023).

4. Summary and conclusions

This comprehensive study provides the first detailed assessment of OA sources and their seasonal dynamics in Delhi and Kanpur, two of India's heavily polluted cities, based on near-molecular level analysis. We quantified eight OA types, four of which were linked to biomass burning. Overall, both cities experienced high contributions from biomass burning, with Kanpur being more affected (66 % of OA) compared to Delhi (35 % of OA). Among these, F-BBOA and A-BBOA, distinguished by their degree of oxygenation, originated from residential biomass uses and were prevalent during the colder months. Another OA type (NOA) was characterized by unique 2N-containing compounds, such as $C_{11}H_{20}N_2$ and $C_{12}H_{22}N_2$, likely derived from alkaloids present in wood or cow dung used for domestic purposes. While these three OA types were mainly linked to local emissions, we also identified an OA type rich in nitro-phenol-like species, associated with a regional transport of agricultural fire emissions (AgrOA). Its concentration peaked during the the harvest season, aligned with rice stubble burning from October to November. The successful identification and direct quantification of AgrOA with relatively low uncertainty provide critical insights into the distinct impacts of open burning, which were previously not separated from other BBOA types. Such observation-based quantitative information is particularly crucial, given the high uncertainties in

air quality models due to incomplete fire emission inventories and insufficient chemical detail. Other anthropogenic activities overall contributed 61 % of OA in Delhi, and 28 % of OA in Kanpur, represented by three additional OA types: fresh emissions from liquid fossil fuel combustion (HOA), urban emissions mixed with aging emissions from traffic and cooking (UOA), and contributions from volatile compounds predominantly affecting Delhi, likely originating from industries within/ surrounding the city (DIOA)—including locally relevant toxic species, exemplified by melamine, which require further attention. Additionally, OA formed from natural biogenic volatile organic compounds, such as mono- and sesquiterpenes, was identified, accounting for 5 % of OA in Delhi, 7 % of OA in Kanpur.

Overall, the short-term exposure to $PM_{2.5}$ was estimated to contribute 6 % of all deaths in both Delhi and Kanpur, averaged across all sampling days. Source-specific acute mortality estimation further underscores the important role of agricultural fire OA originating from distant rural areas. This distinct OA type could account for nearly 50 % of the $PM_{2.5}$-attributable mortality burden in Kanpur, and 32 % in Delhi during the post-monsoon harvest season, largely driven by the intensive fire emission and further aging. These findings illustrate the urgent and critical need for regional cooperative air pollution mitigation strategies, accounting not only for urban emissions but also for stubble residue burning emissions. Despite limitations in the source-specific health impact assessment, our analysis offers valuable insights for policy-makers by improving the quantification of local and transported OA, and emphasizing the importance of health-oriented strategies for cost-effective $PM_{2.5}$ reductions. The findings may also guide other regions facing similarly severe air pollution episodes such as Southeast Asia, and Africa. Future research is needed to quantify the health impacts of specific sources and individual compounds on populations, particularly vulnerable groups, to effectively mitigate $PM_{2.5}$ effects on public health.

CRediT authorship contribution statement

Yufang Hao: Writing – original draft, Writing – review & editing, Conceptualization, Methodology, Data curation, Investigation, Formal analysis, Visualization. **Jan Strähl:** Writing – review & editing, Data curation, Investigation. **Peeyush Khare:** Writing – review & editing, Data curation, Investigation. **Tianqu Cui:** Writing – review & editing, Data curation, Investigation. **Kristty Schneider-Beltran:** Writing – review & editing, Investigation. **Lu. Qi:** Writing – review & editing, Investigation. **Dongyu Wang:** Writing – review & editing, Investigation. **Jens Top:** Writing – review & editing, Investigation. **Mihnea Surdu:** Writing – review & editing, Investigation. **Deepika Bhattu:** Writing – review & editing, Data curation, Investigation. **Himadri Sekhar Bhowmik:** Writing – review & editing. **Pawan Vats:** Writing – review & editing, Investigation. **Pragati Rai:** Writing – review & editing, Investigation. **Varun Kumar:** Writing – review & editing, Investigation. **Dilip Ganguly:** Writing – review & editing, Resources. **Sönke Szidat:** Writing – review & editing, Resources. **Gaëlle Uzu:** Writing – review & editing, Resources. **Jean-Luc Jaffrezo:** Writing – review & editing, Resources. **Rhabira Elazzouzi:** Writing – review & editing, Investigation. **Neeraj Rastogi:** Writing – review & editing, Resources. **Jay Slowik:** Writing – review & editing, Investigation. **Imad EI Haddad:** Writing – review & editing, Conceptualization, Methodology, Supervision, Resources, Funding acquisition. **Sachchida Nand Tripathi:** Writing – review & editing, Resources. **André S.H. Prévôt:** Writing – review & editing, Conceptualization, Methodology, Investigation, Supervision, Resources, Funding acquisition. **Kaspar Rudolf Daellenbach:** Writing – original draft, Writing – review & editing, Conceptualization, Methodology, Investigation, Supervision, Resources, Funding acquisition.

Declaration of competing interest

The authors declare that they have no known competing financial interests or personal relationships that could have appeared to influence the work reported in this paper.

Acknowledgments

The present work was funded by the SDC Clean Air Project in India (grant no. 7F-10093.01.04) from Swiss Agency for Development and Cooperation (SDC) and MOLecular composition of ORGanics in Atmospheric Aging Experiments (MOLORG) (grant no. 200020_188624) from the Swiss National Science Foundation (SNSF). JLJ and GU would like to thank all staff from the Air O Sol analytical plateau at IGE (Grenoble, France) for the measurements performed on filters (EC-OC on Sunset, IC-MS, HPLC-PAD, and ICP-MSMS). S.N.T. acknowledges the support of Central Pollution Control Board, Government of India, and Centre of Excellence (ATMAN) approved by the office of the Principal Scientific Officer to the Government of India. S.N.T. also acknowledges support under J.C. Bose National Fellowship under the aegis of Science and Engineering Research Board, Department of Science and Technology, Government of India and supported by a group of philanthropic funders, including the Bloomberg Philanthropies, the Open Philanthropy. K.R.D. acknowledges support by SNSF Ambizione grant PZPGP2_201992. We also thank for Dr. Hiren T Jethva for providing the permission of the use of fire activities image and useful suggestions.

Appendix A. Supplementary data

Supplementary information to this article can be found online at https://doi.org/10.1016/j.envint.2025.109583.

Data availability

The full dataset used in the figures is publicly available at Zenodo (https://doi.org/10.5281/zenodo.15608527).

References

Aguilera, R., Corringham, T., Gershunov, A., Benmarhnia, T., 2021. Wildfire smoke impacts respiratory health more than fine particles from other sources: observational evidence from Southern California. Nat. Commun. 12, 1493. https://doi.org/10.1038/s41467-021-21708-0.

Al-Kindi, S.S., Pope, F.D., Beddows, D.C., Bloss, W.J., Harrison, R.M., 2016. Size-dependent chemical ageing of oleic acid aerosol under dry and humidified conditions. Atmos. Chem. Phys. 16, 15561–15579. https://doi.org/10.5194/acp-16-15561-2016.

Amato, F., Viana, M., Richard, A., Furger, M., Prévôt, A.S.H., Nava, S., Lucarelli, F., Bukowiecki, N., Alastuey, A., Reche, C., Moreno, T., Pandolfi, M., Pey, J., Querol, X., 2011. Size and time-resolved roadside enrichment of atmospheric particulate pollutants. Atmos. Chem. Phys. 11, 2917–2931. https://doi.org/10.5194/acp-11-2917-2011.

Arora, P., Sharma, D., Kumar, P., Jain, S., 2020. Assessment of clean cooking technologies under different fuel use conditions in rural areas of Northern India. Chemosphere 257, 127315. https://doi.org/10.1016/j.chemosphere.2020.127315.

Arya, S., Rautela, R., Chavan, D., Kumar, S., 2021. Evaluation of soil contamination due to crude E-waste recycling activities in the capital city of India. Process Saf. Environ. Prot. 152, 641–653. https://doi.org/10.1016/j.psep.2021.07.001.

Bai, W., Zhang, L., Yan, L., Wang, X., Zhou, Z., 2023. Crop straw resource utilization as pilot policy in China: an event history analysis. Int. J. Environ. Res. Public Health 20, 3939. https://doi.org/10.3390/ijerph20053939.

Bertrand, A., Stefenelli, G., Jen, C.N., Pieber, S.M., Bruns, E.A., Ni, H., Temime-Roussel, B., Slowik, J.G., Goldstein, A.H., El Haddad, I., Baltensperger, U., Prévôt, A. S.H., Wortham, H., Marchand, N., 2018. Evolution of the chemical fingerprint of biomass burning organic aerosol during aging. Atmos. Chem. Phys. 18, 7607–7624. https://doi.org/10.5194/acp-18-7607-2018.

Bhattu, D., Tripathi, S.N., Bhowmik, H.S., Moschos, V., Lee, C.P., Rauber, M., Salazar, G., Abbaszade, G., Cui, T., Slowik, J.G., Vats, P., Mishra, S., Lalchandani, V., Satish, R., Rai, P., Casotto, R., Tobler, A., Kumar, V., Hao, Y., Qi, L., Khare, P., Manousakas, M. I., Wang, Q., Han, Y., Tian, J., Darfeuil, S., Minguillon, M.C., Hueglin, C., Conil, S., Rastogi, N., Srivastava, A.K., Ganguly, D., Bjelic, S., Canonaco, F., Schnelle-Kreis, J., Dominutti, P.A., Jaffrezo, J.-L., Szidat, S., Chen, Y., Cao, J., Baltensperger, U., Uzu, G., Daellenbach, K.R., El Haddad, I., Prévôt, A.S.H., 2024. Local incomplete combustion emissions define the PM2.5 oxidative potential in Northern India. Nat. Commun. 15, 3517. https://doi.org/10.1038/s41467-024-47785-5.

Bhowmik, H.S., Tripathi, S.N., Puthussery, J.V., Verma, V., Dave, J., Rastogi, N., 2024a. Reactive oxygen species generation from winter water-soluble organic aerosols in Delhi's PM2.5. Atmos. Environ. X 22, 100262. https://doi.org/10.1016/j.aeaoa.2024.100262.

Bhowmik, H.S., Tripathi, S.N., Shukla, A.K., Lalchandani, V., Murari, V., Devaprasad, M., Shivam, A., Bhushan, R., Prévôt, A.S.H., Rastogi, N., 2024b. Contribution of fossil and biomass-derived secondary organic carbon to winter water-soluble organic aerosols in Delhi, India. Sci. Total Environ. 912, 168655. https://doi.org/10.1016/j.scitotenv.2023.168655.

Bikkina, S., Andersson, A., Kirillova, E.N., Holmstrand, H., Tiwari, S., Srivastava, A.K., Bisht, D.S., Gustafsson, Ö., 2019. Air quality in megacity Delhi affected by countryside biomass burning. Nat. Sustain. 2, 200–205. https://doi.org/10.1038/s41893-019-0219-0.

de Bont, J., Krishna, B., Stafoggia, M., Banerjee, T., Dholakia, H., Garg, A., Ingole, V., Jaganathan, S., Kloog, I., Lane, K., Mall, R.K., Mandal, S., Nori-Sarma, A., Prabhakaran, D., Rajiva, A., Tiwari, A.S., Wei, Y., Wellenius, G.A., Schwartz, J., Prabhakaran, P., Ljungman, P., 2024. Ambient air pollution and daily mortality in ten cities of India: a causal modelling study. Lancet Planet. Health 8, e433–e440. https://doi.org/10.1016/S2542-5196(24)00114-1.

Bozzetti, C., Sosedova, Y., Xiao, M., Daellenbach, K.R., Ulevicius, V., Dudoitis, V., Mordas, G., Byčenkienė, S., Plauškaitė, K., Vlachou, A., Golly, B., Chazeau, B., Besombes, J.-L., Baltensperger, U., Jaffrezo, J.-L., Slowik, J.G., El Haddad, I., Prévôt, A.S.H., 2017. Argon offline-AMS source apportionment of organic aerosol over yearly cycles for an urban, rural, and marine site in northern Europe. Atmos. Chem. Phys. 17, 117–141. https://doi.org/10.5194/acp-17-117-2017.

Brege, M., Paglione, M., Gilardoni, S., Decesari, S., Facchini, M.C., Mazzoleni, L.R., 2018. Molecular insights on aging and aqueous-phase processing from ambient biomass burning emissions-influenced Po Valley fog and aerosol. Atmos. Chem. Phys. 18, 13197–13214. https://doi.org/10.5194/acp-18-13197-2018.

Brege, M.A., China, S., Schum, S., Zelenyuk, A., Mazzoleni, L.R., 2021. Extreme molecular complexity resulting in a continuum of carbonaceous species in biomass burning tar balls from wildfire smoke. ACS Earth Space Chem. 5, 2729–2739. https://doi.org/10.1021/acsearthspacechem.1c00141.

Canagaratna, M.R., Jayne, J.T., Jimenez, J.L., Allan, J.D., Alfarra, M.R., Zhang, Q., Onasch, T.B., Drewnick, F., Coe, H., Middlebrook, A., Delia, A., Williams, L.R., Trimborn, A.M., Northway, M.J., DeCarlo, P.F., Kolb, C.E., Davidovits, P., Worsnop, D.R., 2007. Chemical and microphysical characterization of ambient aerosols with the aerodyne aerosol mass spectrometer. Mass Spectrom. Rev. 26, 185–222. https://doi.org/10.1002/mas.20115.

Canonaco, F., Crippa, M., Slowik, J.G., Baltensperger, U., Prévôt, A.S.H., 2013. SoFi, an IGOR-based interface for the efficient use of the generalized multilinear engine (ME-2) for the source apportionment: ME-2 application to aerosol mass spectrometer data. Atmos. Meas. Tech. 6, 3649–3661. https://doi.org/10.5194/amt-6-3649-2013.

Canonaco, F., Tobler, A., Chen, G., Sosedova, Y., Slowik, J.G., Bozzetti, C., Daellenbach, K.R., El Haddad, I., Crippa, M., Huang, R.-J., Furger, M., Baltensperger, U., Prévôt, A.S.H., 2021. A new method for long-term source apportionment with time-dependent factor profiles and uncertainty assessment using SoFi pro: application to 1 year of organic aerosol data. Atmos. Meas. Tech. 14, 923–943. https://doi.org/10.5194/amt-14-923-2021.

Carpenter, B., Gelman, A., Hoffman, M.D., Lee, D., Goodrich, B., Betancourt, M., Brubaker, M., Guo, J., Li, P., Riddell, A., 2017. Stan: a probabilistic programming language. J. Stat. Softw. 76, 1–32. https://doi.org/10.18637/jss.v076.i01.

Cash, J.M., Langford, B., Di Marco, C., Mullinger, N.J., Allan, J., Reyes-Villegas, E., Joshi, R., Heal, M.R., Acton, W.J.F., Hewitt, C.N., Misztal, P.K., Drysdale, W., Mandal, T.K., Shivani, G., Gurjar, B.R., Nemitz, E., 2021. Seasonal analysis of submicron aerosol in Old Delhi using high-resolution aerosol mass spectrometry: chemical characterisation, source apportionment and new marker identification. Atmos. Chem. Phys. 21, 10133–10158. https://doi.org/10.5194/acp-21-10133-2021.

Casotto, R., Cvitešić Kušan, A., Bhattu, D., Cui, T., Manousakas, M.I., Frka, S., Kroflič, A., Grgić, I., Ciglenečki, I., Baltensperger, U., Slowik, J.G., Daellenbach, K.R., Prévôt, A.S.H., 2022. Chemical composition and sources of organic aerosol on the Adriatic coast in Croatia. Atmos. Environ. X 13, 100159. https://doi.org/10.1016/j.aeaoa.2022.100159.

Chanchani, D., Oskarsson, P., 2021. 'If the gas runs out, we are not going to sleep hungry': exploring household energy choices in India's critically polluted coal belt. Energy Res. Soc. Sci. 80, 102181. https://doi.org/10.1016/j.erss.2021.102181.

Chen, G., Guo, Y., Yue, X., Tong, S., Gasparrini, A., Bell, M.L., Armstrong, B., Schwartz, J., Jaakkola, J.J.K., Zanobetti, A., Lavigne, E., Saldiva, P.H.N., Kan, H., Royé, D., Milojevic, A., Overcenco, A., Urban, A., Schneider, A., Entezari, A., Vicedo-Cabrera, A.M., Zeka, A., Tobias, A., Nunes, B., Alahmad, B., Forsberg, B., Pan, S.-C., Íñiguez, C., Ameling, C., la C. Valencia, C.D., Åström, C., Houthuijs, D., Dung, D.V., Samoli, E., Mayvaneh, F., Sera, F., Carrasco-Escobar, G., Lei, Y., Orru, H., Kim, H., Holobaca, I.-H., Kyselý, J., Teixeira, J.P., Madureira, J., Katsouyanni, K., Hurtado-Díaz, M., Maasikmets, M., Ragettli, M.S., Hashizume, M., Stafoggia, M., Pascal, M., Scortichini, M., de S.Z.S. Coêlho, M., Ortega, N.V., Ryti, N.R.I., Scovronick, N., Matus, P., Goodman, P., Garland, R.M., Abrutzky, R., Garcia, S.O., Rao, S., Fratianni, S., Dang, T.N., Colistro, V., Huber, V., Lee, W., Seposo, X., Honda, Y., Guo, Y.L., Ye, T., Yu, W., Abramson, M.J., Samet, J.M., Li, S., 2021. Mortality risk attributable to wildfire-related PM2·5 pollution: a global time series study in 749 locations. Lancet Planet. Health 5, e579–e587. https://doi.org/10.1016/S2542-5196(21)00200-X.

Chen, Y., Takeuchi, M., Nah, T., Xu, L., Canagaratna, M.R., Stark, H., Baumann, K., Canonaco, F., Prévôt, A.S.H., Huey, L.G., Weber, R.J., Ng, N.L., 2020. Chemical characterization of secondary organic aerosol at a rural site in the southeastern US: insights from simultaneous high-resolution time-of-flight aerosol mass spectrometer (HR-ToF-AMS) and FIGAERO chemical ionization mass spectrometer (CIMS) measurements. Atmos. Chem. Phys. 20, 8421–8440. https://doi.org/10.5194/acp-20-8421-2020.

Chowdhury, S., Dey, S., Guttikunda, S., Pillarisetti, A., Smith, K.R., Di Girolamo, L., 2019. Indian annual ambient air quality standard is achievable by completely mitigating emissions from household sources. Proc. Natl. Acad. Sci. 116, 10711–10716. https://doi.org/10.1073/pnas.1900888116.

Cook, R.D., Lin, Y.-H., Peng, Z., Boone, E., Chu, R.K., Dukett, J.E., Gunsch, M.J., Zhang, W., Tolic, N., Laskin, A., Pratt, K.A., 2017. Biogenic, urban, and wildfire influences on the molecular composition of dissolved organic compounds in cloud water. Atmos. Chem. Phys. 17, 15167–15180. https://doi.org/10.5194/acp-17-15167-2017.

Cui, T., Manousakas, M.I., Wang, Q., Uzu, G., Hao, Y., Khare, P., Qi, L., Chen, Y., Han, Y., Slowik, J.G., Jaffrezo, J.-L., Cao, J., Prévôt, A.S.H., Daellenbach, K.R., 2024. Composition and sources of organic aerosol in two megacities in Western China using complementary mass spectrometric and statistical techniques. ACS EST Air. https://doi.org/10.1021/acsestair.4c00051.

Daellenbach, K.R., Bozzetti, C., Křepelová, A., Canonaco, F., Wolf, R., Zotter, P., Fermo, P., Crippa, M., Slowik, J.G., Sosedova, Y., Zhang, Y., Huang, R.-J., Poulain, L., Szidat, S., Baltensperger, U., El Haddad, I., Prévôt, A.S.H., 2016. Characterization and source apportionment of organic aerosol using offline aerosol mass spectrometry. Atmos. Meas. Tech. 9, 23–39. https://doi.org/10.5194/amt-9-23-2016.

Daellenbach, K.R., Stefenelli, G., Bozzetti, C., Vlachou, A., Fermo, P., Gonzalez, R., Piazzalunga, A., Colombi, C., Canonaco, F., Hueglin, C., Kasper-Giebl, A., Jaffrezo, J.-L., Bianchi, F., Slowik, J.G., Baltensperger, U., El-Haddad, I., Prévôt, A.S.H., 2017. Long-term chemical analysis and organic aerosol source apportionment at nine sites in central Europe: source identification and uncertainty assessment. Atmos. Chem. Phys. 17, 13265–13282. https://doi.org/10.5194/acp-17-13265-2017.

de Foy, B., Cui, Y.Y., Schauer, J.J., Janssen, M., Turner, J.R., Wiedinmyer, C., 2015. Estimating sources of elemental and organic carbon and their temporal emission patterns using a least squares inverse model and hourly measurements from the St. Louis-midwest supersite. Atmos. Chem. Phys. 15, 2405–2427. https://doi.org/10.5194/acp-15-2405-2015.

De Haan, D.O., Hawkins, L.N., Kononenko, J.A., Turley, J.J., Corrigan, A.L., Tolbert, M.A., Jimenez, J.L., 2011. Formation of nitrogen-containing oligomers by methylglyoxal and amines in simulated evaporating cloud droplets. Environ. Sci. Technol. 45, 984–991. https://doi.org/10.1021/es102933x.

Deshpande, N.R., Kulkarni, A., Krishna Kumar, K., 2012. Characteristic features of hourly rainfall in India. Int. J. Climatol. 32, 1730–1744. https://doi.org/10.1002/joc.2375.

Devi, N.L., Kumar, A., Yadav, I.C., 2020. PM10 and PM2.5 in Indo-Gangetic Plain (IGP) of India: chemical characterization, source analysis, and transport pathways. Urban Clim. 33, 100663. https://doi.org/10.1016/j.uclim.2020.100663.

Dutta, A., Patra, A., Hazra, K.K., Nath, C.P., Kumar, N., Rakshit, A., 2022. A state of the art review in crop residue burning in India: previous knowledge, present circumstances and future strategies. Environ. Chall. 8, 100581. https://doi.org/10.1016/j.envc.2022.100581.

Dutta, M., Chatterjee, A., 2022. A deep insight into state-level aerosol pollution in India: long-term (2005–2019) characteristics, source apportionment, and future projection (2023). Atmos. Environ. 289, 119312. https://doi.org/10.1016/j.atmosenv.2022.119312.

Faisal, M., Hazarika, N., Ganguly, D., Kumar, M., Singh, V., 2022. PM2.5 bound species variation and source characterization in the post-lockdown period of the Covid-19 pandemic in Delhi. Urban Clim. 46, 101290. https://doi.org/10.1016/j.uclim.2022.101290.

Fang, Z., Lai, A., Cai, D., Li, C., Carmieli, R., Chen, J., Wang, X., Rudich, Y., 2024. Secondary organic aerosol generated from biomass burning emitted phenolic compounds: oxidative potential, reactive oxygen species, and cytotoxicity. Environ. Sci. Technol. 58, 8194–8206. https://doi.org/10.1021/acs.est.3c09903.

Fleming, L.T., Lin, P., Laskin, A., Laskin, J., Weltman, R., Edwards, R.D., Arora, N.K., Yadav, A., Meinardi, S., Blake, D.R., Pillarisetti, A., Smith, K.R., Nizkorodov, S.A., 2018. Molecular composition of particulate matter emissions from dung and brushwood burning household cookstoves in Haryana, India. Atmos. Chem. Phys. 18, 2461–2480. https://doi.org/10.5194/acp-18-2461-2018.

Fleming, L.T., Lin, P., Roberts, J.M., Selimovic, V., Yokelson, R., Laskin, J., Laskin, A., Nizkorodov, S.A., 2020. Molecular composition and photochemical lifetimes of brown carbon chromophores in biomass burning organic aerosol. Atmos. Chem. Phys. 20, 1105–1129. https://doi.org/10.5194/acp-20-1105-2020.

Fountoukis, C., Nenes, A., 2007. ISORROPIA II: a computationally efficient thermodynamic equilibrium model for K^+–Ca^{2+}–Mg^{2+}–NH_4^+–Na^+–SO_4^{2-}––NO_3^-–Cl^-–H_2O aerosols. Atmos. Chem. Phys. Discuss. 7, 1893–1939. https://doi.org/10.5194/acpd-7-1893-2007.

Fu, T.-M., Jacob, D.J., Wittrock, F., Burrows, J.P., Vrekoussis, M., Henze, D.K., 2008. Global budgets of atmospheric glyoxal and methylglyoxal, and implications for formation of secondary organic aerosols. J. Geophys. Res. Atmos. 113. https://doi.org/10.1029/2007JD009505.

Fuller, R., Landrigan, P.J., Balakrishnan, K., Bathan, G., Bose-O'Reilly, S., Brauer, M., Caravanos, J., Chiles, T., Cohen, A., Corra, L., Cropper, M., Ferraro, G., Hanna, J., Hanrahan, D., Hu, H., Hunter, D., Janata, G., Kupka, R., Lanphear, B., Lichtveld, M., Martin, K., Mustapha, A., Sanchez-Triana, E., Sandilya, K., Schaefli, L., Shaw, J., Seddon, J., Suk, W., Téllez-Rojo, M.M., Yan, C., 2022. Pollution and health: a progress update. Lancet Planet. Health 6, e535–e547. https://doi.org/10.1016/S2542-5196(22)00090-0.

Gan, Y., Lu, X., Chen, S., Jiang, X., Yang, S., Ma, X., Li, M., Yang, F., Shi, Y., Wang, X., 2024. Aqueous-phase formation of N-containing secondary organic compounds affected by the ionic strength. J. Environ. Sci. 138, 88–101. https://doi.org/10.1016/j.jes.2023.03.003.

Gangwar, C., Choudhari, R., Chauhan, A., Kumar, A., Singh, A., Tripathi, A., 2019. Assessment of air pollution caused by illegal e-waste burning to evaluate the human health risk. Environ. Int. 125, 191–199. https://doi.org/10.1016/j.envint.2018.11.051.

Garsa, K., Khan, A.A., Jindal, P., Middey, A., Luqman, N., Mohanty, H., Tiwari, S., 2023. Assessment of meteorological parameters on air pollution variability over Delhi. Environ. Monit. Assess. 195, 1315. https://doi.org/10.1007/s10661-023-11922-2.

GBD 2019 Risk Factors Collaborators, 2020. Global burden of 87 risk factors in 204 countries and territories, 1990-2019: a systematic analysis for the Global Burden of Disease Study 2019. Lancet Lond. Engl. 396, 1223–1249. https://doi.org/10.1016/S0140-6736(20)30752-2.

Glojek, K., Dinh Ngoc Thuy, V., Weber, S., Uzu, G., Manousakas, M., Elazzouzi, R., Džepina, K., Darfeuil, S., Ginot, P., Jaffrezo, J.L., Žabkar, R., Turšič, J., Podkoritnik, A., Močnik, G., 2024. Annual variation of source contributions to PM10 and oxidative potential in a mountainous area with traffic, biomass burning, cement-plant and biogenic influences. Environ. Int. 189, 108787. https://doi.org/10.1016/j.envint.2024.108787.

Goetz, J.D., Giordano, M.R., Stockwell, C.E., Bhave, P.V., Puppala, P.S., Panday, A.K., Jayarathne, T., Stone, E.A., Yokelson, R.J., DeCarlo, P.F., 2022. Aerosol mass spectral profiles from NAMaSTE field-sampled south asian combustion sources. ACS Earth Space Chem. 6, 2619–2631. https://doi.org/10.1021/acsearthspacechem.2c00173.

Goyal, P., Gulia, S., Goyal, S.K., 2025. Critical review of air pollution contribution in Delhi due to paddy stubble burning in North Indian States. Atmos. Environ. 346, 121058. https://doi.org/10.1016/j.atmosenv.2025.121058.

Gunthe, S.S., Liu, P., Panda, U., Raj, S.S., Sharma, A., Darbyshire, E., Reyes-Villegas, E., Allan, J., Chen, Y., Wang, X., Song, S., Pöhlker, M.L., Shi, L., Wang, Y., Kommula, S. M., Liu, T., Ravikrishna, R., McFiggans, G., Mickley, L.J., Martin, S.T., Pöschl, U., Andreae, M.O., Coe, H., 2021. Enhanced aerosol particle growth sustained by high continental chlorine emission in India. Nat. Geosci. 14, 77–84. https://doi.org/10.1038/s41561-020-00677-x.

He, Y., Zhao, B., Wang, S., Valorso, R., Chang, X., Yin, D., Feng, B., Camredon, M., Aumont, B., Dearden, A., Jathar, S.H., Shrivastava, M., Jiang, Z., Cappa, C.D., Yee, L. D., Seinfeld, J.H., Hao, J., Donahue, N.M., 2024. Formation of secondary organic aerosol from wildfire emissions enhanced by long-time ageing. Nat. Geosci. 17, 124–129. https://doi.org/10.1038/s41561-023-01355-4.

Hemann, J.G., Brinkman, G.L., Dutton, S.J., Hannigan, M.P., Milford, J.B., Miller, S.L., 2009. Assessing positive matrix factorization model fit: a new method to estimate uncertainty and bias in factor contributions at the measurement time scale. Atmos. Chem. Phys. 9, 497–513. https://doi.org/10.5194/acp-9-497-2009.

Hennigan, C.J., Sullivan, A.P., Collett Jr., J.L., Robinson, A.L., 2010. Levoglucosan stability in biomass burning particles exposed to hydroxyl radicals. Geophys. Res. Lett. 37. https://doi.org/10.1029/2010GL043088.

Collaborators, I.-L., 2021. Health and economic impact of air pollution in the states of India: the Global Burden of Disease Study 2019. Lancet Planet. Health 5, e25–e38. https://doi.org/10.1016/S2542-5196(20)30298-9.

Jain, S., Sharma, S.K., Vijayan, N., Mandal, T.K., 2020. Seasonal characteristics of aerosols (PM2.5 and PM10) and their source apportionment using PMF: a four year study over Delhi. India. Environ. Pollut. 262, 114337. https://doi.org/10.1016/j.envpol.2020.114337.

Jawaa, Z.T., Biswas, K.F., Khan, M.F., Moniruzzaman, M., 2024. Source and respiratory deposition of trace elements in PM2.5 at an urban location in Dhaka city. Heliyon 10, e25420. https://doi.org/10.1016/j.heliyon.2024.e25420.

Joo, T., Rogers, M.J., Soong, C., Hass-Mitchell, T., Heo, S., Bell, M.L., Ng, N.L., Gentner, D.R., 2024. Aged and obscured wildfire smoke associated with downwind health risks. Environ. Sci. Technol. Lett. https://doi.org/10.1021/acs.estlett.4c00785.

Kajino, M., Ishijima, K., Ching, J., Yamaji, K., Ishikawa, R., Kajikawa, T., Singh, T., Nakayama, T., Matsumi, Y., Kojima, K., Patra, P.K., Hayashida, S., 2024. Impact of post monsoon crop residue burning on $PM_{2.5}$ over North India: optimizing emissions using a high-density in situ surface observation network. EGUsphere 1–40. https://doi.org/10.5194/egusphere-2024-1811.

Kant, Y., Chauhan, P., Natwariya, A., Kannaujiya, S., Mitra, D., 2022. Long term influence of groundwater preservation policy on stubble burning and air pollution over North-West India. Sci. Rep. 12, 2090. https://doi.org/10.1038/s41598-022-06043-8.

Kaskaoutis, D.G., Kumar, S., Sharma, D., Singh, R.P., Kharol, S.K., Sharma, M., Singh, A. K., Singh, S., Singh, A., Singh, D., 2014. Effects of crop residue burning on aerosol properties, plume characteristics, and long-range transport over northern India. J. Geophys. Res. Atmos. 119, 5424–5444. https://doi.org/10.1002/2013JD021357.

Keil, A., Krishnapriya, P.P., Mitra, A., Jat, M.L., Sidhu, H.S., Krishna, V.V., Shyamsundar, P., 2021. Changing agricultural stubble burning practices in the Indo-Gangetic plains: is the Happy Seeder a profitable alternative? Int. J. Agric. Sustain. 19, 128–151. https://doi.org/10.1080/14735903.2020.1834277.

Kulkarni, S.H., Ghude, S.D., Jena, C., Karumuri, R.K., Sinha, B., Sinha, V., Kumar, R., Soni, V.K., Khare, M., 2020. How much does large-scale crop residue burning affect the air quality in Delhi? Environ. Sci. Technol. 54, 4790–4799. https://doi.org/10.1021/acs.est.0c00329.

Kumar, B., Chakraborty, A., Tripathi, N., Bhattu, D., 2016. Highly time resolved chemical characterization of submicron organic aerosols at a polluted urban location. Environ. Sci. Process. Impacts 18, 1285–1296. https://doi.org/10.1039/C6EM00392C.

Kumar, V., Giannoukos, S., Haslett, S.L., Tong, Y., Singh, A., Bertrand, A., Lee, C.P., Wang, D.S., Bhattu, D., Stefenelli, G., Dave, J.S., Puthussery, J.V., Qi, L., Vats, P., Rai, P., Casotto, R., Satish, R., Mishra, S., Pospisilova, V., Mohr, C., Bell, D.M., Ganguly, D., Verma, V., Rastogi, N., Baltensperger, U., Tripathi, S.N., Prévôt, A.S.H., Slowik, J.G., 2022. Highly time-resolved chemical speciation and source apportionment of organic aerosol components in Delhi, India, using extractive electrospray ionization mass spectrometry. Atmos. Chem. Phys. 22, 7739–7761. https://doi.org/10.5194/acp-22-7739-2022.

Lakra, A., Shukla, A.K., Bhowmik, H.S., Yadav, A.K., Jain, V., Murari, V., Gaddamidi, S., Lalchandani, V., Tripathi, S.N., 2024. Comparative analysis of winter composite-PM2.5 in Central Indo Gangetic Plain cities: combined organic and inorganic source apportionment and characterization, with a focus on the photochemical age effect on secondary organic aerosol formation. Atmos. Environ. 338, 120827. https://doi.org/10.1016/j.atmosenv.2024.120827.

Lan, R., Eastham, S.D., Liu, T., Norford, L.K., Barrett, S.R.H., 2022. Air quality impacts of crop residue burning in India and mitigation alternatives. Nat. Commun. 13, 6537. https://doi.org/10.1038/s41467-022-34093-z.

Laskin, A., Smith, J.S., Laskin, J., 2009. Molecular characterization of nitrogen-containing organic compounds in biomass burning aerosols using high-resolution mass spectrometry. Environ. Sci. Technol. 43, 3764–3771. https://doi.org/10.1021/es803456n.

Li, J., Gao, X., He, Y., Wang, L., Wang, Y., Zeng, L., 2022. Elevated emissions of melamine and its derivatives in the indoor environments of typical e-waste recycling facilities and adjacent communities and implications for human exposure. J. Hazard. Mater. 432, 128652. https://doi.org/10.1016/j.jhazmat.2022.128652.

Li, K., Zhang, J., Bell, D.M., Wang, T., Lamkaddam, H., Cui, T., Qi, L., Surdu, M., Wang, D., Du, L., El Haddad, I., Slowik, J.G., Prevot, A.S.H., 2024. Uncovering the dominant contribution of intermediate volatility compounds in secondary organic aerosol formation from biomass-burning emissions. Natl. Sci. Rev. 11, nwae014. https://doi.org/10.1093/nsr/nwae014.

Li, R., Zhang, K., Li, Q., Yang, L., Wang, S., Liu, Z., Zhang, X., Chen, H., Yi, Y., Feng, J., Wang, Q., Huang, L., Wang, W., Wang, Y., Yu, J.Z., Li, L., 2023a. Characteristics and degradation of organic aerosols from cooking sources based on hourly observations of organic molecular markers in urban environments. Atmos. Chem. Phys. 23, 3065–3081. https://doi.org/10.5194/acp-23-3065-2023.

Li, Y., Fu, T.-M., Yu, J.Z., Yu, X., Chen, Q., Miao, R., Zhou, Y., Zhang, A., Ye, J., Yang, X., Tao, S., Liu, H., Yao, W., 2023b. Dissecting the contributions of organic nitrogen aerosols to global atmospheric nitrogen deposition and implications for ecosystems. Natl. Sci. Rev. 10, nwad244. https://doi.org/10.1093/nsr/nwad244.

Lin, P., Rincon, A.G., Kalberer, M., Yu, J.Z., 2012. Elemental composition of HULIS in the Pearl River Delta Region, China: results inferred from positive and negative electrospray high resolution mass spectrometric data. Environ. Sci. Technol. 46, 7454–7462. https://doi.org/10.1021/es300285d.

Liu, C., Chen, R., Sera, F., Vicedo-Cabrera, A.M., Guo, Y., Tong, S., Coelho, M.S.Z.S., Saldiva, P.H.N., Lavigne, E., Matus, P., Valdes Ortega, N., Osorio Garcia, S., Pascal, M., Stafoggia, M., Scortichini, M., Hashizume, M., Honda, Y., Hurtado-Díaz, M., Cruz, J., Nunes, B., Teixeira, J.P., Kim, H., Tobias, A., Íñiguez, C., Forsberg, B., Åström, C., Ragettli, M.S., Guo, Y.-L., Chen, B.-Y., Bell, M.L., Wright, C. Y., Scovronick, N., Garland, R.M., Milojevic, A., Kyselý, J., Urban, A., Orru, H., Indermitte, E., Jaakkola, J.J.K., Ryti, N.R.I., Katsouyanni, K., Analitis, A., Zanobetti, A., Schwartz, J., Chen, J., Wu, T., Cohen, A., Gasparrini, A., Kan, H., 2019. Ambient particulate air pollution and daily mortality in 652 cities. N. Engl. J. Med. 381, 705–715. https://doi.org/10.1056/NEJMoa1817364.

Liu, T., Mickley, L.J., Patel, P.N., Gautam, R., Jain, M., Singh, S., DeFries, R.S., Marlier, M.E., 2022. Cascading delays in the monsoon rice growing season and postmonsoon agricultural fires likely exacerbate air pollution in North India. J. Geophys. Res. Atmospheres 127, e2022JD036790. https://doi.org/10.1029/2022JD036790.

Lütjens, L.H., Pawlowski, S., Silvani, M., Blumenstein, U., Richter, I., 2023. Melamine in the environment: a critical review of available information. Environ. Sci. Eur. 35, 2. https://doi.org/10.1186/s12302-022-00707-y.

Madhu, A., Jang, M., Deacon, D., 2023. Modeling the influence of chain length on secondary organic aerosol (SOA) formation via multiphase reactions of alkanes. Atmos. Chem. Phys. 23, 1661–1675. https://doi.org/10.5194/acp-23-1661-2023.

Maheshwarkar, P., Ralhan, A., Sunder Raman, R., Tibrewal, K., Venkataraman, C., Dhandapani, A., Kumar, R.N., Mukherjee, S., Chatterje, A., Rabha, S., Saikia, B.K., Bhardwaj, A., Chaudhary, P., Sinha, B., Lokhande, P., Phuleria, H.C., Roy, S., Imran, M., Habib, G., Azharuddin Hashmi, M., Qureshi, A., Qadri, A.M., Gupta, T., Lian, Y., Pandithurai, G., Prasad, L., Murthy, S., Deswal, M., Laura, J.S., Chhangani, A.K., Najar, T.A., Jehangir, A., 2022. Understanding the influence of meteorology and emission sources on PM2.5 mass concentrations across India: first results from the COALESCE network. J. Geophys. Res. Atmos 127, e2021JD035663. https://doi.org/10.1029/2021JD035663.

Manchanda, C., Kumar, M., Singh, V., 2022. Meteorology governs the variation of Delhi's high particulate-bound chloride levels. Chemosphere 291, 132879. https://doi.org/10.1016/j.chemosphere.2021.132879.

Mishra, N.K., Biswas, P., Patel, S., 2024. Future of clean energy for cooking in India: a comprehensive analysis of fuel alternatives. Energy Sustain. Dev. 81, 101500. https://doi.org/10.1016/j.esd.2024.101500.

Mishra, S., Tripathi, S.N., Kanawade, V.P., Haslett, S.L., Dada, L., Ciarelli, G., Kumar, V., Singh, A., Bhattu, D., Rastogi, N., Daellenbach, K.R., Ganguly, D., Gargava, P., Slowik, J.G., Kulmala, M., Mohr, C., El-Haddad, I., Prevot, A.S.H., 2023. Rapid night-time nanoparticle growth in Delhi driven by biomass-burning emissions. Nat. Geosci. 16, 224–230. https://doi.org/10.1038/s41561-023-01138-x.

Mohr, C., DeCarlo, P.F., Heringa, M.F., Chirico, R., Slowik, J.G., Richter, R., Reche, C., Alastuey, A., Querol, X., Seco, R., Peñuelas, J., Jiménez, J.L., Crippa, M., Zimmermann, R., Baltensperger, U., Prévôt, A.S.H., 2012. Identification and quantification of organic aerosol from cooking and other sources in Barcelona using aerosol mass spectrometer data. Atmos. Chem. Phys. 12, 1649–1665. https://doi.org/10.5194/acp-12-1649-2012.

Montes, C., Sapkota, T., Singh, B., 2022. Seasonal patterns in rice and wheat residue burning and surface PM2.5 concentration in northern India. Atmos. Environ. X 13, 100154. https://doi.org/10.1016/j.aeaoa.2022.100154.

Mukherjee, A., Tripathi, S.N., Ram, K., Saha, D., 2023. New Delhi air potentially chokes from groundwater conservation policies in adjoining regions. Environ. Sci. Technol. Lett. 10, 3–5. https://doi.org/10.1021/acs.estlett.2c00848.

Navinya, C., Kapoor, T.S., Anurag, G., Lokhande, P., Sharma, R., Kumari, J., Habib, G., Arya, R., Mandal, T.K., Muthalagu, A., Qureshi, A., Najar, T.A., Jehangir, A., Jain, S., Goel, A., Rabha, S., Saikia, B.K., Chaudhary, P., Sinha, B., Haswani, D., Raman, R.S., Dhandapani, A., Iqbal, J., Mukherjee, S., Chatterjee, A., Lian, Y., Pandithurai, G., Venkataraman, C., Phuleria, H.C., 2023. Heating and lighting: understanding overlooked energy-consumption activities in the Indian residential sector. Environ. Res. Commun. 5, 045004. https://doi.org/10.1088/2515-7620/acca6f.

Nguyen, T.B., Bateman, A.P., Bones, D.L., Nizkorodov, S.A., Laskin, J., Laskin, A., 2010. High-resolution mass spectrometry analysis of secondary organic aerosol generated by ozonolysis of isoprene. Atmos. Environ. 44, 1032–1042. https://doi.org/10.1016/j.atmosenv.2009.12.019.

Niu, X., Li, J., Wang, Q., Ho, S.S.H., Sun, J., Li, L., Cao, J., Ho, K.F., 2020. Characteristics of fresh and aged volatile organic compounds from open burning of crop residues. Sci. Total Environ. 726, 138545. https://doi.org/10.1016/j.scitotenv.2020.138545.

Paatero, P., Tapper, U., 1994. Positive matrix factorization: a non-negative factor model with optimal utilization of error estimates of data values. Environmetrics 5, 111–126. https://doi.org/10.1002/env.3170050203.

Patel, K., Bhandari, S., Gani, S., Campmier, M.J., Kumar, P., Habib, G., Apte, J., Hildebrandt Ruiz, L., 2021. Sources and dynamics of submicron aerosol during the autumn onset of the air pollution season in Delhi, India. ACS Earth Space Chem. 5, 118–128. https://doi.org/10.1021/acsearthspacechem.0c00340.

Pawar, H., Sinha, B., 2022. Residential heating emissions (can) exceed paddy-residue burning emissions in rural northwest India. Atmos. Environ. 269, 118846. https://doi.org/10.1016/j.atmosenv.2021.118846.

Pisso, I., Sollum, E., Grythe, H., Kristiansen, N.I., Cassiani, M., Eckhardt, S., Arnold, D., Morton, D., Thompson, R.L., Groot Zwaaftink, C.D., Evangeliou, N., Sodemann, H., Haimberger, L., Henne, S., Brunner, D., Burkhart, J.F., Fouilloux, A., Brioude, J., Philipp, A., Seibert, P., Stohl, A., 2019. The Lagrangian particle dispersion model FLEXPART version 10.4. Geosci. Model Dev. 12, 4955–4997. https://doi.org/10.5194/gmd-12-4955-2019.

Qi, L., Chen, M., Stefenelli, G., Pospisilova, V., Tong, Y., Bertrand, A., Hueglin, C., Ge, X., Baltensperger, U., Prévôt, A.S.H., Slowik, J.G., 2019. Organic aerosol source apportionment in Zurich using an extractive electrospray ionization time-of-flight mass spectrometer (EESI-TOF-MS) – Part 2: biomass burning influences in winter. Atmos. Chem. Phys. 19, 8037–8062. https://doi.org/10.5194/acp-19-8037-2019.

Qi, L., Vogel, A.L., Esmaeilirad, S., Cao, L., Zheng, J., Jaffrezo, J.-L., Fermo, P., Kasper-Giebl, A., Daellenbach, K.R., Chen, M., Ge, X., Baltensperger, U., Prévôt, A.S.H., Slowik, J.G., 2020. A 1-year characterization of organic aerosol composition and sources using an extractive electrospray ionization time-of-flight mass spectrometer (EESI-TOF). Atmos. Chem. Phys. 20, 7875–7893. https://doi.org/10.5194/acp-20-7875-2020.

Rai, P., Furger, M., El Haddad, I., Kumar, V., Wang, L., Singh, A., Dixit, K., Bhattu, D., Petit, J.-E., Ganguly, D., Rastogi, N., Baltensperger, U., Tripathi, S.N., Slowik, J.G., Prévôt, A.S.H., 2020. Real-time measurement and source apportionment of elements in Delhi's atmosphere. Sci. Total Environ. 742, 140332. https://doi.org/10.1016/j.scitotenv.2020.140332.

Rajput, P., Singh, D.K., Singh, A.K., Gupta, T., 2018. Chemical composition and source-apportionment of sub-micron particles during wintertime over Northern India: new insights on influence of fog-processing. Environ. Pollut. 233, 81–91. https://doi.org/10.1016/j.envpol.2017.10.036.

Ravindra, K., Singh, T., Sinha, V., Sinha, B., Paul, S., Attri, S.D., Mor, S., 2021. Appraisal of regional haze event and its relationship with PM2.5 concentration, crop residue burning and meteorology in Chandigarh, India. Chemosphere 273, 128562. https://doi.org/10.1016/j.chemosphere.2020.128562.

Saini, P., Sharma, M., 2020. Cause and age-specific premature mortality attributable to PM2.5 exposure: an analysis for million-plus Indian cities. Sci. Total Environ. 710, 135230. https://doi.org/10.1016/j.scitotenv.2019.135230.

Sang, S., Chu, C., Zhang, T., Chen, H., Yang, X., 2022. The global burden of disease attributable to ambient fine particulate matter in 204 countries and territories, 1990–2019: a systematic analysis of the Global Burden of Disease Study 2019. Ecotoxicol. Environ. Saf. 238, 113588. https://doi.org/10.1016/j.ecoenv.2022.113588.

Sarkar, S., Singh, R.P., Chauhan, A., 2018. Crop residue burning in northern India: increasing threat to greater India. J. Geophys. Res. Atmospheres 123, 6920–6934. https://doi.org/10.1029/2018JD028428.

Saxena, P., Kumar, A., Muzammil, M., Bojjagani, S., Patel, D.K., Kumari, A., Khan, A.H., Kisku, G.C., 2024. Spatio-temporal distribution and source contributions of the ambient pollutants in Lucknow city. India. Environ. Monit. Assess. 196, 693. https://doi.org/10.1007/s10661-024-12832-7.

Schneider, E., Czech, H., Popovicheva, O., Chichaeva, M., Kobelev, V., Kasimov, N., Minkina, T., Rüger, C.P., Zimmermann, R., 2024. Mass spectrometric analysis of unprecedented high levels of carbonaceous aerosol particles long-range transported from wildfires in the Siberian Arctic. Atmos. Chem. Phys. 24, 553–576. https://doi.org/10.5194/acp-24-553-2024.

Sharma, D., Jain, S., 2019. Impact of intervention of biomass cookstove technologies and kitchen characteristics on indoor air quality and human exposure in rural settings of India. Environ. Int. 123, 240–255. https://doi.org/10.1016/j.envint.2018.11.059.

Singh, T., Matsumi, Y., Nakayama, T., Hayashida, S., Patra, P.K., Yasutomi, N., Kajino, M., Yamaji, K., Khatri, P., Takigawa, M., Araki, H., Kurogi, Y., Kuji, M., Muramatsu, K., Imasu, R., Ananda, A., Arbain, A.A., Ravindra, K., Bhardwaj, S., Kumar, S., Mor, S., Dhaka, S.K., Dimri, A.P., Sharma, A., Singh, N., Bhatti, M.S., Yadav, R., Vatta, K., Mor, S., 2023. Very high particulate pollution over northwest India captured by a high-density in situ sensor network. Sci. Rep. 13, 13201. https://doi.org/10.1038/s41598-023-39471-1.

Singh, V., Singh, S., Biswal, A., 2021. Exceedances and trends of particulate matter (PM2.5) in five Indian megacities. Sci. Total Environ. 750, 141461. https://doi.org/10.1016/j.scitotenv.2020.141461.

Srinivas, B., Sarin, M.M., 2014. $PM_{2.5}$, EC and OC in atmospheric outflow from the Indo-Gangetic Plain: temporal variability and aerosol organic carbon-to-organic mass conversion factor. Sci. Total Environ. 487, 196–205. https://doi.org/10.1016/j.scitotenv.2014.04.002.

Stefenelli, G., Pospisilova, V., Lopez-Hilfiker, F.D., Daellenbach, K.R., Hüglin, C., Tong, Y., Baltensperger, U., Prévôt, A.S.H., Slowik, J.G., 2019. Organic aerosol source apportionment in Zurich using an extractive electrospray ionization time-of-flight mass spectrometer (EESI-TOF-MS) – Part 1: biogenic influences and day–night chemistry in summer. Atmos. Chem. Phys. 19, 14825–14848. https://doi.org/10.5194/acp-19-14825-2019.

Tobler, A., Bhattu, D., Canonaco, F., Lalchandani, V., Shukla, A., Thamban, N.M., Mishra, S., Srivastava, A.K., Bisht, D.S., Tiwari, S., Singh, S., Močnik, G., Baltensperger, U., Tripathi, S.N., Slowik, J.G., Prévôt, A.S.H., 2020. Chemical characterization of PM2.5 and source apportionment of organic aerosol in New Delhi, India. Sci. Total Environ. 745, 140924. https://doi.org/10.1016/j.scitotenv.2020.140924.

Tong, Y., Pospisilova, V., Qi, L., Duan, J., Gu, Y., Kumar, V., Rai, P., Stefenelli, G., Wang, L., Wang, Y., Zhong, H., Baltensperger, U., Cao, J., Huang, R.-J., Prévôt, A.S.H., Slowik, J.G., 2021. Quantification of solid fuel combustion and aqueous chemistry contributions to secondary organic aerosol during wintertime haze events in Beijing. Atmos. Chem. Phys. 21, 9859–9886. https://doi.org/10.5194/acp-21-9859-2021.

Vadrevu, K.P., Ellicott, E., Badarinath, K.V.S., Vermote, E., 2011. MODIS derived fire characteristics and aerosol optical depth variations during the agricultural residue burning season, north India. Environ. Pollut. 159, 1560–1569. https://doi.org/10.1016/j.envpol.2011.03.001.

Vasilakopoulou, C.N., Matrali, A., Skyllakou, K., Georgopoulou, M., Aktypis, A., Florou, K., Kaltsonoudis, C., Siouti, E., Kostenidou, E., Błaziak, A., Nenes, A., Papagiannis, S., Eleftheriadis, K., Patoulias, D., Kioutsioukis, I., Pandis, S.N., 2023. Rapid transformation of wildfire emissions to harmful background aerosol. NPJ Clim. Atmos. Sci. 6, 1–9. https://doi.org/10.1038/s41612-023-00544-7.

Wang, S., Gallimore, P.J., Liu-Kang, C., Yeung, K., Campbell, S.J., Utinger, B., Liu, T., Peng, H., Kalberer, M., Chan, A.W.H., Abbatt, J.P.D., 2023. Dynamic wood smoke aerosol toxicity during oxidative atmospheric aging. Environ. Sci. Technol. 57, 1246–1256. https://doi.org/10.1021/acs.est.2c05929.

Wang, Y., Hu, M., Lin, P., Guo, Q., Wu, Z., Li, M., Zeng, L., Song, Y., Zeng, L., Wu, Y., Guo, S., Huang, X., He, L., 2017. Molecular Characterization of nitrogen-containing organic compounds in humic-like substances emitted from straw residue burning. Environ. Sci. Technol. 51, 5951–5961. https://doi.org/10.1021/acs.est.7b00248.

Wang, Y., Hu, M., Lin, P., Tan, T., Li, M., Xu, N., Zheng, J., Du, Z., Qin, Y., Wu, Y., Lu, S., Song, Y., Wu, Z., Guo, S., Zeng, L., Huang, X., He, L., 2019. Enhancement in particulate organic nitrogen and light absorption of humic-like substances over Tibetan Plateau due to long-range transported biomass burning emissions. Environ. Sci. Technol. 53, 14222–14232. https://doi.org/10.1021/acs.est.9b06152.

Watanabe, M., Nakata, C., Wu, W., Kawamoto, K., Noma, Y., 2007. Characterization of semi-volatile organic compounds emitted during heating of nitrogen-containing plastics at low temperature. Chemosphere 68, 2063–2072. https://doi.org/10.1016/j.chemosphere.2007.02.022.

Weltgesundheitsorganisation, Organization, W.H., 2021. WHO global air quality guidelines: particulate matter (PM2.5 and PM10), ozone, nitrogen dioxide, sulfur dioxide and carbon monoxide. World Health Organization.

Williams, L.R., Gonzalez, L.A., Peck, J., Trimborn, D., McInnis, J., Farrar, M.R., Moore, K. D., Jayne, J.T., Robinson, W.A., Lewis, D.K., Onasch, T.B., Canagaratna, M.R., Trimborn, A., Timko, M.T., Magoon, G., Deng, R., Tang, D., de la Rosa Blanco, E., Prévôt, A.S.H., Smith, K.A., Worsnop, D.R., 2013. Characterization of an aerodynamic lens for transmitting particles greater than 1 micrometer in diameter into the aerodyne aerosol mass spectrometer. Atmos. Meas. Tech. 6, 3271–3280. https://doi.org/10.5194/amt-6-3271-2013.

Wu, X., Vu, T.V., Shi, Z., Harrison, R.M., Liu, D., Cen, K., 2018. Characterization and source apportionment of carbonaceous PM2.5 particles in China – a review. Atmos. Environ. 189, 187–212. https://doi.org/10.1016/j.atmosenv.2018.06.025.

Xiao, Y., Hu, M., Li, X., Zong, T., Xu, N., Hu, S., Zeng, L., Chen, S., Song, Y., Guo, S., Wu, Z., 2022. Aqueous secondary organic aerosol formation attributed to phenols from biomass burning. Sci. Total Environ. 847, 157582. https://doi.org/10.1016/j.scitotenv.2022.157582.

Yazdani, A., Takahama, S., Kodros, J.K., Paglione, M., Masiol, M., Squizzato, S., Florou, K., Kaltsonoudis, C., Jorga, S.D., Pandis, S.N., Nenes, A., 2023. Chemical evolution of primary and secondary biomass burning aerosols during daytime and nighttime. Atmos. Chem. Phys. 23, 7461–7477. https://doi.org/10.5194/acp-23-7461-2023.

Ye, T., Xu, R., Yue, X., Chen, G., Yu, P., Coêlho, M.S.Z.S., Saldiva, P.H.N., Abramson, M. J., Guo, Y., Li, S., 2022. Short-term exposure to wildfire-related PM2.5 increases mortality risks and burdens in Brazil. Nat. Commun. 13, 7651. https://doi.org/10.1038/s41467-022-35326-x.

Yu, L., Smith, J., Laskin, A., George, K.M., Anastasio, C., Laskin, J., Dillner, A.M., Zhang, Q., 2016. Molecular transformations of phenolic SOA during photochemical aging in the aqueous phase: competition among oligomerization, functionalization, and fragmentation. Atmos. Chem. Phys. 16, 4511–4527. https://doi.org/10.5194/acp-16-4511-2016.

Yu, W., Xu, R., Ye, T., Abramson, M.J., Morawska, L., Jalaludin, B., Johnston, F.H., Henderson, S.B., Knibbs, L.D., Morgan, G.G., Lavigne, E., Heyworth, J., Hales, S., Marks, G.B., Woodward, A., Bell, M.L., Samet, J.M., Song, J., Li, S., Guo, Y., 2024. Estimates of global mortality burden associated with short-term exposure to fine particulate matter (PM2·5). Lancet Planet. Health 8, e146–e155. https://doi.org/10.1016/S2542-5196(24)00003-2.

Zhang, J., Li, K., Wang, T., Gammelsæter, E., Cheung, R.K.Y., Surdu, M., Bogler, S., Bhattu, D., Wang, D.S., Cui, T., Qi, L., Lamkaddam, H., El Haddad, I., Slowik, J.G., Prevot, A.S.H., Bell, D.M., 2023. Bulk and molecular-level composition of primary organic aerosol from wood, straw, cow dung, and plastic burning. Atmos. Chem. Phys. 23, 14561–14576. https://doi.org/10.5194/acp-23-14561-2023.

Zhang, J., Zuend, A., Top, J., Surdu, M., El Haddad, I., Slowik, J.G., Prevot, A.S.H., Bell, D.M., 2024. Estimation of the volatility and apparent activity coefficient of Levoglucosan in wood-burning organic aerosols. Environ. Sci. Technol. Lett. 11, 1214–1219. https://doi.org/10.1021/acs.estlett.4c00608.

Zhao, M., Wang, K., 2024. Short-term effects of PM2.5 components on the respiratory infectious disease: a global perspective. Environ. Geochem. Health 46, 293. https://doi.org/10.1007/s10653-024-02024-0.

Zięba, A., Ramza, P., 2011. Standard deviation of the mean of autocorrelated observations estimated with the use of the autocorrelation function estimated from the data. Metrol. Meas. Syst. 18, 529–542.